ARTICLE

Functional interplay between NF-κB-inducing kinase and c-Abl kinases limits response to Aurora inhibitors in multiple myeloma

Laura Mazzera,[1,2] Manuela Abeltino,[1] Guerino Lombardi,[2] Anna Maria Cantoni,[3] Roberto Ria,[4] Micaela Ricca,[2] Ilaria Saltarella,[4] Valeria Naponelli,[1] Federica Maria Angela Rizzi,[1,5] Roberto Perris,[5,6] Attilio Corradi,[3] Angelo Vacca,[4] Antonio Bonati[1,5] and Paolo Lunghi[5,6]

[1]Department of Medicine and Surgery, University of Parma, Parma; [2]Istituto Zooprofilattico Sperimentale della Lombardia e dell'Emilia Romagna "Bruno Ubertini," Brescia; [3]Department of Veterinary Science, University of Parma, Parma; [4]Department of Biomedical Sciences and Human Oncology, Section of Internal Medicine and Clinical Oncology, University of Bari "Aldo Moro" Medical School, Bari; [5]Center for Molecular and Translational Oncology, University of Parma, Parma and [6]Department of Chemistry, Life Sciences and Environmental Sustainability, University of Parma, Parma, Italy

Ferrata Storti Foundation

Haematologica 2019
Volume 104(12):2465-2481

ABSTRACT

Considering that Aurora kinase inhibitors are currently under clinical investigation in hematologic cancers, the identification of molecular events that limit the response to such agents is essential for enhancing clinical outcomes. Here, we discover a NF-κB-inducing kinase (NIK)-c-Abl-STAT3 signaling-centered feedback loop that restrains the efficacy of Aurora inhibitors in multiple myeloma. Mechanistically, we demonstrate that Aurora inhibition promotes NIK protein stabilization *via* downregulation of its negative regulator TRAF2. Accumulated NIK converts c-Abl tyrosine kinase from a nuclear proapoptotic into a cytoplasmic antiapoptotic effector by inducing its phosphorylation at Thr735, Tyr245 and Tyr412 residues, and, by entering into a trimeric complex formation with c-Abl and STAT3, increases both the transcriptional activity of STAT3 and expression of the antiapoptotic STAT3 target genes PIM1 and PIM2. This consequently promotes cell survival and limits the response to Aurora inhibition. The functional disruption of any of the components of the trimer NIK-c-Abl-STAT3 or the PIM survival kinases consistently enhances the responsiveness of myeloma cells to Aurora inhibitors. Importantly, concurrent inhibition of NIK or c-Abl disrupts Aurora inhibitor-induced feedback activation of STAT3 and sensitizes myeloma cells to Aurora inhibitors, implicating a combined inhibition of Aurora and NIK or c-Abl kinases as potential therapies for multiple myeloma. Accordingly, pharmacological inhibition of c-Abl together with Aurora resulted in substantial cell death and tumor regression *in vivo*. The findings reveal an important functional interaction between NIK, Abl and Aurora kinases, and identify the NIK, c-Abl and PIM survival kinases as potential pharmacological targets for improving the efficacy of Aurora inhibitors in myeloma.

Introduction

Despite encouraging advances in therapy, multiple myeloma (MM) remains an incurable disease due to complex genomic alterations, lower sensitivity to chemotherapy of MM cells in the bone marrow microenvironment, and the emergence of drug resistance.[1]

Recent genetic evidence has established a pathogenetic role for NF-κB signaling in MM.[2-4] In particular, at various frequencies, MM cells harbor gain-of-function mutations as well as loss-of-function mutations in genes encoding components of the classical and the alternative NF-κB pathways.[2-4] Among these, mutations in the genes encoding NF-κB-inducing kinase (NIK) or its negative regulators TRAF2,

Correspondence:

PAOLO LUNGHI
p.lunghi@libero.it

Received: Ocrtober 17, 2018.

Accepted: April 3, 2019.

Pre-published: April 4, 2019.

doi:10.3324/haematol.2018.208280

Check the online version for the most updated information on this article, online supplements, and information on authorship & disclosures: www.haematologica.org/content/104/12/2465

TRAF3, cIAP1, and cIAP2 lead to increased stability of NIK and subsequent aberrant activation of the non-canonical and canonical NF-κB pathways.[2-7]

In addition to regulating NF-κB pathways, the NIK signaling pathway has been demonstrated to crosstalk with and activate other critical cancer-associated pathways including the MAPK-ERK[8,9] and JAK/STAT3.[10] Moreover, these pathways are highly interconnected at many levels, and have been demonstrated to be often persistently and simultaneously activated in many human cancers, including myeloma.[11,12]

NF-κB and STAT3 signaling can also be regulated by c-Abl,[13,14] a ubiquitously expressed non-receptor tyrosine kinase that plays an important role in regulating critical cellular processes, including proliferation, survival, apoptosis, differentiation, invasion, adhesion, migration, and stress responses.[15,16]

The tyrosine kinase c-Abl has been reported to have opposing and antagonistic functions in the regulation of cell proliferation and survival depending on its subcellular localization, phosphorylation state, and cellular context.[17] In particular, activation of cytoplasmic c-Abl in response to growth factors, cytokines and Src tyrosine kinases, can promote mitogenic and survival signals,[17,18] whereas activation of nuclear c-Abl in response to DNA damage can negatively regulate cell proliferation and mediate apoptosis/necrosis.[15]

The subcellular localization of c-Abl is critically controlled by binding with the 14-3-3 protein, which requires the phosphorylation of c-Abl at an amino acid residue Thr735.[19]

Wild-type c-Abl is localized both in the nucleus and cytoplasm, in contrast to its oncogenic forms that are localized exclusively in the cytoplasm. Oncogenic forms of c-Abl exhibit enhanced kinase and transforming activities and play a critical role in the pathogenesis of chronic and acute leukemias.[20] MM cells display high levels of nuclear c-Abl in response to ongoing DNA damage and genomic instability.[21,22] However, most of its nuclear tumor suppressor functions are compromised because of the disruption of the ABL-YAP1-p73 axis.[21]

In MM and other hematologic and solid malignancies, genomic instability, centrosome amplification and aneuploidy have been associated with the overexpression of Aurora kinases, a family of serine/threonine kinases that play essential and distinct roles in mitosis.[23]

In addition to their mitosis specific substrates, Aurora kinases have also been found to functionally interact with proteins involved in critical cancer-associated pathways including NF-κB, STAT3 and DNA-damage response pathways.[24-27] On the basis of these findings, Aurora kinases have been considered as therapeutic targets for cancer and Aurora kinases inhibitors (AKI) have been extensively explored. These have shown encouraging pre-clinical and early clinical activity in different cancer types either alone or in combination with other agents.[25,28-31] Unfortunately, AKI have not proved to be sufficiently effective and/or caused too many adverse side-effects in myeloma patients, both when used as monotherapy or in combination with other targeted therapy agents.[29-31] The poor efficacy of AKI therapies in MM may, in part, be related to the still undetermined drug-induced compensatory mechanisms occurring in both the MM cells and their microenvironment, and, consequently, to the lack of appropriate mechanism-based combination therapies.

In this study, we demonstrate that pan-AKI generate pro-survival signals in MM cells by inducing the expression/activation of the pro-survival serine/threonine kinases PIM1 and PIM2[32] through a NIK/c-Abl-mediated activation of STAT3, a cascade of molecular events that consequently limit the response to pan-AKI. Our findings reveal a novel functional interplay between NIK and c-Abl with implications for treatment of MM. They therefore provide the rationale for targeting c-Abl as a novel strategy to enhance activity of Pan-AKI.

Methods

Reagents

Pan-AKI MK-0457 (Merck & Co. Rahway, NJ, USA); pan-AKI PHA-680632 (Pfizer/Nerviano, Italy); pan-AKI AMG-900 (Cayman Chemical Company; Ann Arbor, MI, USA); NIK inhibitor isoquinoline-1,3(2H,4H)-dione (Santa Cruz Biotechnology, Santa Cruz, CA, USA); proteasome inhibitor bortezomib (PS-341) from Janssen-Cilag (Milan, Italy); c-Abl inhibitors imatinib mesylate and nilotinib (Novartis Pharmaceuticals, Basel, Switzerland). STAT3 inhibitor Stattic (6-Nitrobenzo [b]thiophene-1,1-dioxide) and pan-PIM kinase inhibitor SMI-4A (5Z)-5-[[3-(Trifluoromethyl)-phenyl]-methylene]-2,4-thiazolidinedione (Sigma-Aldrich, St. Louis, MO, USA).

Cell cultures

Cell cultures were: human myeloma cell lines (HMCL) OPM-2, U266, RPMI-8226 and JJN3 (DSMZ, Braunschweig, Germany); multidrug-resistant RPMI-8226/R5 HMCL was established as previously described;[33] human bone marrow-derived stromal cell line HS-5 (ATCC, Manassas, VA, USA). Primary MM cells from MM patients and peripheral blood mononuclear cells (PBMC) of healthy subjects were isolated and treated as described in the *Online Supplementary Methods*. The study was approved by the Ethics Committee of the University of Bari "Aldo Moro" (identification n. 5143/2017), and all patients and healthy donors provided informed consent in accordance with the Declaration of Helsinki.

Apoptosis assays, siRNA and plasmid transfections, molecular and statistical analysis

These methods have been previously published[34] and are described in the *Online Supplementary Methods*.

Animal studies, histology, immunohistochemistry and immunofluorescence

The animal study was approved by the Istituto Zooprofilattico Sperimentale della Lombardia e dell'Emilia Romagna review board (n. PRC 2009018). Five-week old non-obese diabetic (NOD) severe combined immunodeficiency (SCID) NOD.CB17-Prkdcscid/J (NOD-SCID) mice (Jackson Laboratory, Bar Harbour, ME, USA) were maintained under the same specific pathogen-free conditions. Histological, immunohistochemical and immunofluorescent studies are described in the *Online Supplementary Methods*.

Results

Pharmacological blockade of Aurora kinases elevates NF-κB-inducing kinase protein levels through TRAF2 degradation

Although pan-AKI were able to prevent TRAIL-induced canonical and non-canonical NF-κB activation, they proved to be only partially effective in reducing the basal NF-κB activity of MM cells.[25] Based on these observations,

we formulated the hypothesis that NIK, a kinase capable of activating both the alternative and classical NF-κB pathways through IKKα/β phosphorylation,[2-4] could interfere with the inhibitory effects of pan-AKI on NF-κB signaling.[24,25]

To investigate this hypothesis, we blocked Aurora kinase activity with the pan-AKI MK-0457 or PHA-680632,[25,29] and monitored the impact on NIK levels in HMCL with barely detectable (OPM-2), very low (U266), low (8226 and R5), or high (JJN3) NIK expression.[2-4] Interestingly, pan-AKI significantly increased NIK protein levels in all the tested HMCL, although to varying degrees depending on the cell line examined, with an average fold increase ranging from 1.3 (U266) to 7.8 (OPM-2) (Figure 1A). Furthermore, consistent with previous studies demonstrating that MM-microenvironmental interactions induce reciprocal activation of NF-κB in both cellular compartments,[35] together with the fact that NIK stabilization is a critical step for NF-κB activation in MM cells,[2-4] we found that adherence of MM cells to HS-5 stromal cells caused a significant accumulation of NIK protein in 4 of 5 HMCL tested (except JJN3) and also in the HS-5 stromal cells, and that this increment was further enhanced by pan-AKI treatment in both the co-cultured cell populations, MM and stromal cells (Figure 1B). Notably, pan-AKI did not significantly affect NIK mRNA levels in MM cells (Figure 1C), thereby suggesting that pan-AKI-induced NIK protein accumulation in MM cells is mainly due to post-translational rather than transcriptional regulation.

Given the critical role of TRAF2 and TRAF3 in regulat-

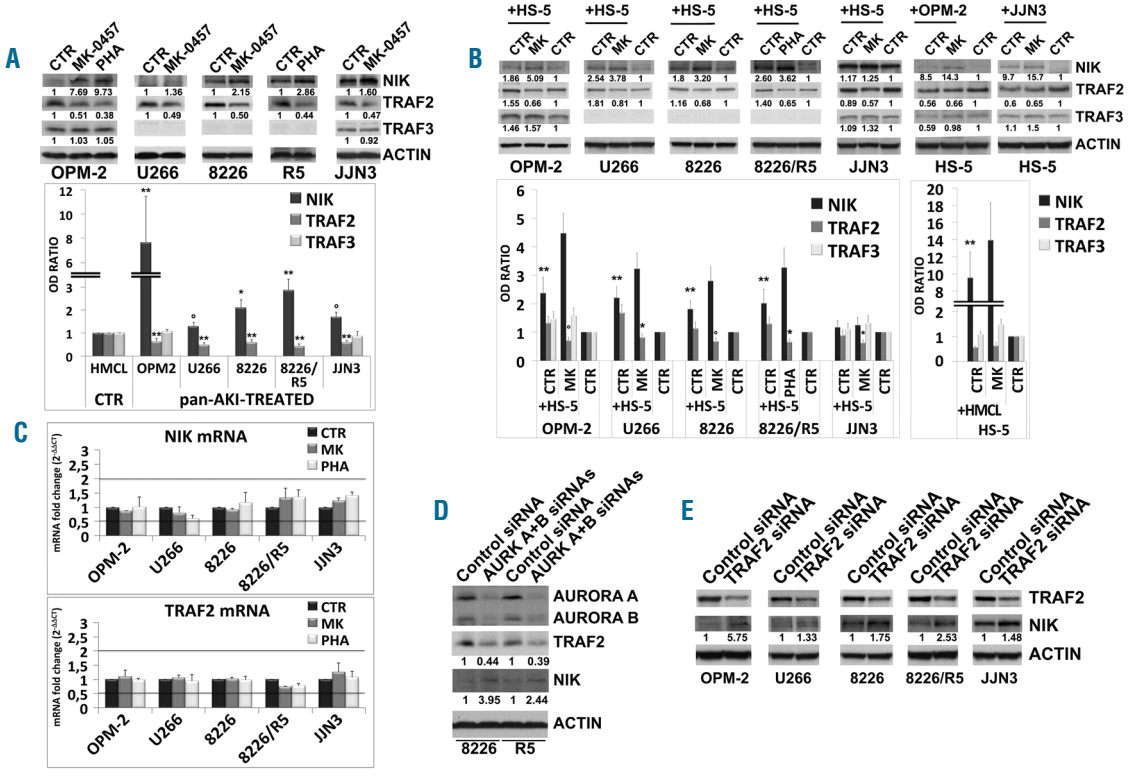

Figure. 1. Aurora kinases inhibition enhances NF-κB-inducing kinase (NIK) expression through TRAF2 degradation. (A) Western blot analysis of endogenous NIK, TRAF2 and TRAF3 proteins in multiple myeloma (MM) cell lines treated for 24 hours (h) with MK-0457 (0.4 μM) or PHA-680632 (1 μM); anti-Actin immunoblotting was performed as loading control. Bands were subjected to densitometric scanning using the TINA 2 software and the ratio of NIK to Actin, TRAF2 to Actin and TRAF3 to Actin was calculated. The relative fold change of protein levels was normalized with respect to the level of the untreated control, which was taken as 1, and is shown under each lane. Histogram represents the mean±Standard Deviation (SD) of six independent experiments (Tukey-Kramer test, °P<0.05, *P<0.005, **P<0.001). (B) MM cell lines were incubated with MK-0457 (0.4 μM) or PHA-680632 (1 μM) in presence or absence of human bone marrow-derived stromal cell line HS-5 (see *Online Supplementary Methods*). After 24 h, MM cell lines were separated from HS-5, lysed and subjected to western blot analysis to monitor the expression of NIK, TRAF2, TRAF3 and Actin as loading control. Bands were then subjected to densitometric analysis as described above and the relative fold change of protein levels was normalized with respect to the level of the untreated control in absence of HS-5, which was taken as 1, and is shown under each lane. In the same way, western blot and densitometry analysis of NIK, TRAF2 and TRAF3 were performed in HS-5 stromal cells separated from co-culture with OPM-2 and JJN3 cells. (Bottom) Changes (folds increase or decrease) in the levels of each protein relative to untreated control in absence of HS-5, which was taken as 1; the histograms represent the mean±SD of 3 independent experiments (Dunnett test, °P<0.05; *P<0.01; **P<0.005). (C) MM cell lines were incubated with MK-0457 (0.4 μM) or PHA-680632 (1 μM) and after 24 h RNA was purified and the expression levels of NIK and TRAF2 mRNA were determined by RT-qPCR in untreated (CTR), MK- and PHA-treated cells. The relative mRNA fold change in treated versus untreated cells was calculated by the $2^{-\Delta\Delta CT}$ method. Results are expressed as mean±SD of two independent determinations. Relative mRNA fold changes comprised between 0.5 and 2 (indicated with black lines) are not considered biologically relevant. (D) RPMI-8226 and 8226/R5 cells were transfected with siRNA against Aurora A and Aurora B (AURK A+B) or unrelated non-specific control siRNA. Forty-eight hours after siRNA transfection MM cell lines were subjected to western blot analysis to monitor the expression of Aurora A, Aurora B, TRAF2, NIK and Actin as loading control. TRAF2 and NIK bands were then subjected to densitometric scanning and the number below each lane represents the relative amount of TRAF2 and NIK normalized to Actin. Protein expression under control siRNA conditions was set as 1 for comparison. (E) MM cell lines were electroporated with non-specific control siRNA or with TRAF2 siRNA. After 24 h, lysates from control or TRAF2 siRNA-transfected MM cells were subjected to western blot analysis to monitor the expression of TRAF2 and NIK; anti-Actin immunoblotting was performed as loading control. The number below each lane represents changes (folds increase) in the levels of NIK in TRAF-2 siRNA relative to control siRNA condition which was set as 1 for comparison.

ing cIAP1/2-mediated NIK proteasomal degradation,[2-7] we investigated the effects of pan-AKI on the protein expression of these NIK negative regulators. We found that pan-AKI treatment induced a significant reduction in the protein levels of TRAF2 but not TRAF3 in all the tested HMCL, either cultured alone (Figure 1A) or co-cultured with HS-5 stromal cells (Figure 1B). Furthermore, pan-AKI treatment did not modulate TRAF2 mRNA levels in MM cells (Figure 1C), thereby indicating that its protein expression is not regulated at transcriptional levels by these inhibitors.

Furthermore, small interfering RNA (siRNA)-mediated knockdown of Aurora-A and -B recapitulated the ability of pan-AKI to down-regulate the negative regulator of NIK, TRAF2, and increase NIK protein levels (Figure 1D), thereby confirming the significant role of Aurora kinases in modulating NIK stability through TRAF2 in MM cells. On the other hand, siRNA-mediated knockdown of TRAF2 led to NIK accumulation in all the HMCL studied (Figure 1E and *Online Supplementary Figure S1*), including those with deletion or inactivating mutations of *TRAF3* (U266, 8226 and 8226/R5) or bearing alterations in the *TRAF3*-binding domain of NIK (JJN3),[2,3] thereby confirming the important role of TRAF2 in regulating NIK degradation in MM.[2,4]

NF-κB-inducing kinase attenuates the anti-tumor activity of pan-AKI in multiple myeloma cells

We found that NIK inhibition by either the NIK small-molecule inhibitor 4H-isoquinoline-1,3-dione (NIK-in)[36] or the NIK-specific siRNA significantly enhanced pan-AKI-induced cell death in all the HMCL tested, either cultured

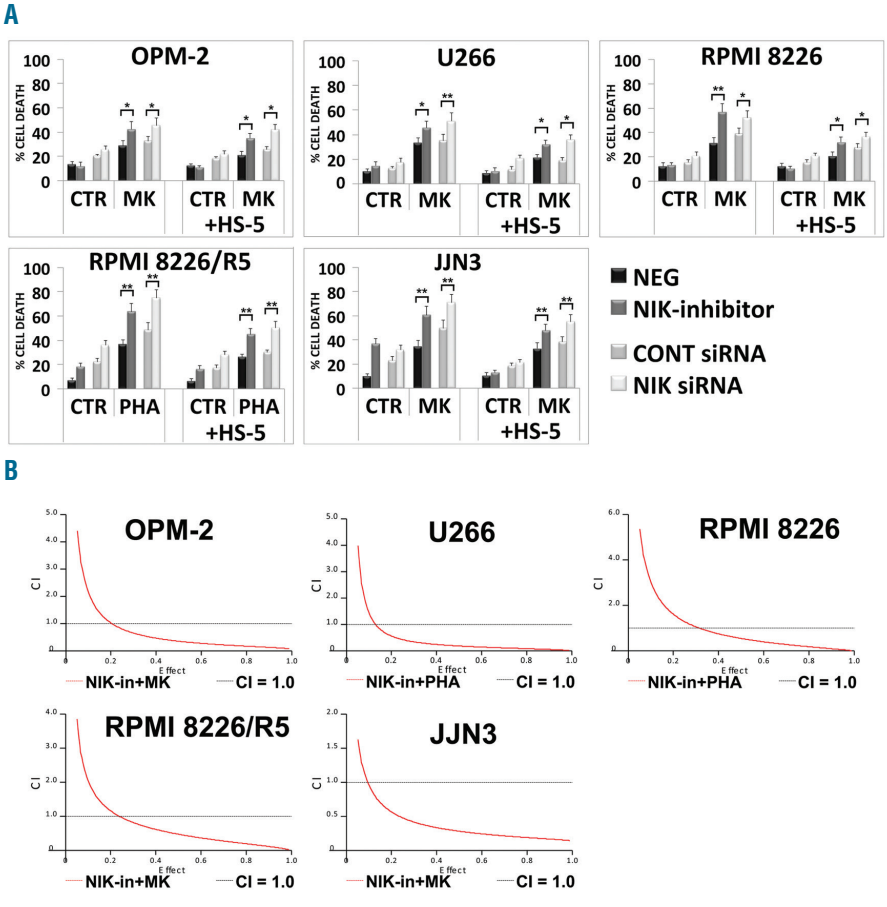

Figure 2. NF-κB-inducing kinase (NIK) inhibition sensitizes multiple myeloma (MM) cells to pan-AKI-induced cell death. (A) MM cell lines were incubated with the NIK inhibitor (NIK-in) at 10 μM or were transfected with NIK siRNA and after 3 hours (h) MM cell lines were treated with MK-0457 (0.4 μM) or PHA-680632 (1 μM) in absence or presence of HS-5 cells (+HS-5) (see Online Supplementary Methods). After 48 h, cell death was measured by annexin-V labeling. Values represent means±Standard Deviation (SD) of four independent experiments. (Dunnett and Tukey-Kramer tests, **P*<0.05; ***P*<0.01 *vs.* MK-0457 treatment). (B) MM cell lines were treated sequentially with escalating doses of the NIK inhibitor (NIK-in) (1-20 μM) for 3 h and subsequently with MK-0457 (0.1-1 μM) or PHA-680632 (0.1-2 μM) alone or in combination with the NIK inhibitor at a fixed ratio indicated in *Online Supplementary Table S1*. After 48 h, cell death was measured by annexin V labeling and the Combination Index values (CI) were calculated using the Chou-Talalay method and Calcusyn software, and the isobologram plots were constructed. CI<1.0 indicate synergism, CI=1.0 indicate additive effect, and CI>1.0 indicate an antagonistic effect. (C) CD138-purified plasma cells from ten patients with MM seeded in presence of HS-5 cells and peripheral blood mononuclear cells (PBMC) from five healthy volunteers were incubated with the NIK inhibitor (NIK-in) at 10 μM for 3 h and then were treated with MK-0457 (0.4 μM) or PHA-680632 (1 μM). After 24 h, cell death was measured by annexin-V staining or sub-G1 DNA content. Because of heterogeneous levels of basal cell death, the data of all ten primary samples and PBMC tested are expressed as % of specific cell death with the formula % Specific cell death = 100 x (induced cell death−basal cell death)/(100−basal cell death) and are shown in box plot format (median line in box delimited by 25th and 75th) (**P*<0.005 *vs.* either treatment alone; Dunnett test).

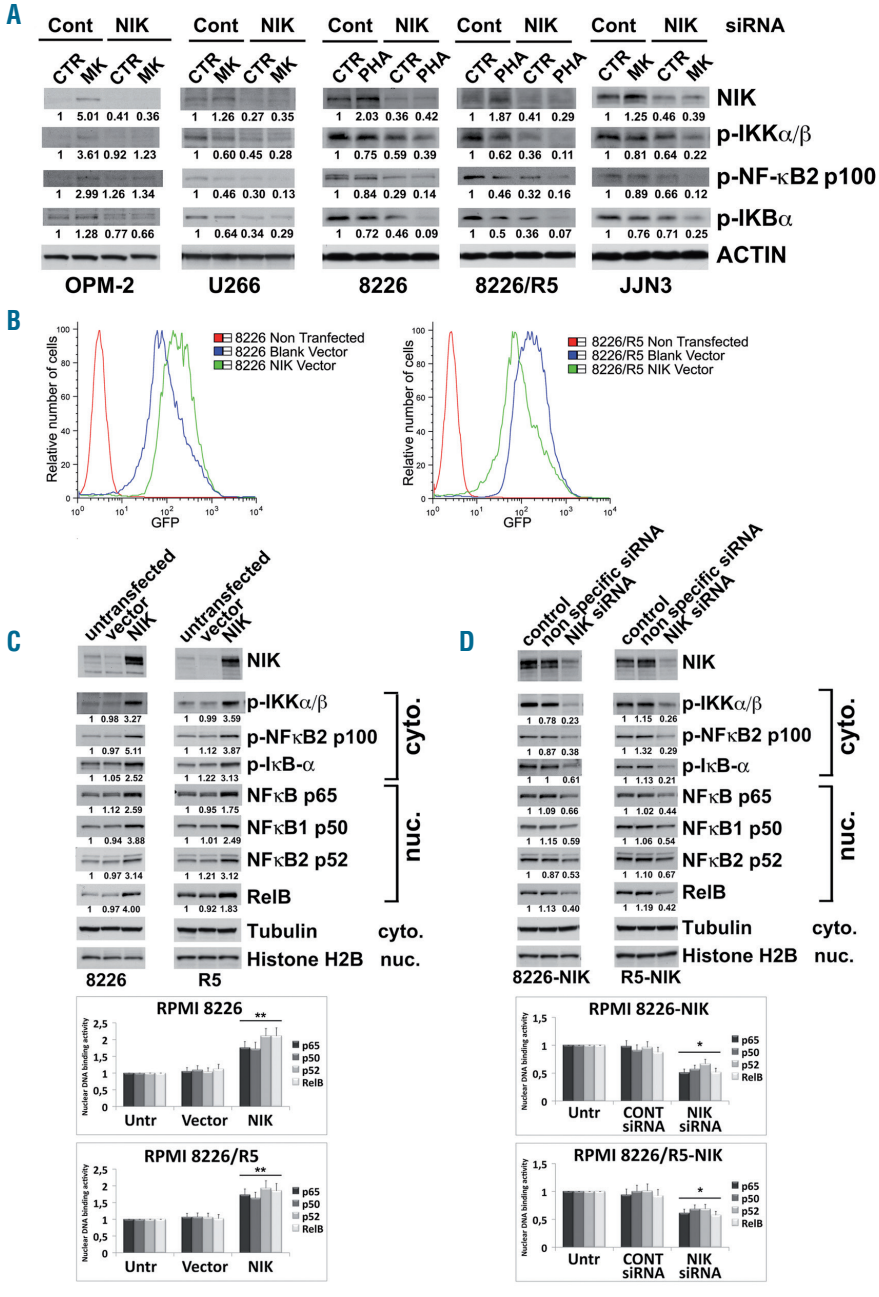

Figure 3. NF-κB-inducing kinase (NIK) accumulation interferes with inhibitory activities of pan-AKI NF–κB. (A) siRNA silencing of NIK but not the non-specific control siRNA, led to a decrease in NIK protein expression. Three hours (h) after electroporation, multiple myeloma (MM) cell lines were treated with the pan-AKI MK-0457 (0.4 μM) or PHA-680632 (1 μM). After 48 h, MM cell lines were lysed and subjected to western blot analysis to monitor the expression of NIK, phospho-IKKα/β, phospho-NF-κB2 p100, phospho-IκBα and Actin as loading control. All western blotting results were evaluated by densitometric scanning, corrected with respect to Actin expression, and expressed relative to the value obtained with the corresponding control set as 1. The relative protein amount is reported below the lanes. (B) RPMI-8226 and 8226/R5 were stably transfected with an empty vector or with plasmid expressing NIK protein. Pools of stable clones (8226-NIK and 8226/R5-NIK) were obtained by selection with puromycin. Both expression vectors co-expressed GFP to monitor the transfection by flow cytometry. Plots represent GFP fluorescence of cells transfected with empty vector (Blank) or that encoding for NIK compared to non-transfected cells. (C) NIK overexpression enhances nuclear localization and DNA transactivation activity of NF-κB subunits. Stable clones of RPMI-8226 and 8226/R5 transfected with empty vector (Blank) or expressing NIK protein or untransfected cells were seeded at a density of $2x10^5$ cells/mL. After 24 h cytoplasmic and nuclear extracts were prepared using the Active Motif's Nuclear Extract Kit. Cytoplasmic cell lysates were immunoblotted against NIK, p-IKKα/β, p-NF-κB2, p-IκB-α and tubulin as marker of cytoplasmic separation as well as loading control; nuclear extracts were immunoblotted against NF-κB p65, NF-κB1 p50, NF-κB2 p52, RelB and histone H2B as nuclear loading control; bands were subjected to densitometric scanning and the number below each lane represents the relative amount of the indicated proteins normalized to tubulin or histone H2B expression. Graphs below represent DNA binding activity of the NF-κB p65, NF-κB1 p50, NF-κB2 p52 and RelB subunit from the same nuclear extracts (TransAM NF-κB ELISA kit); results were normalized to the untransfected control (Untr). Values represent mean±Standard Deviation (SD) of three separate experiments. (**P<0.01 *vs.* untransfected condition; Dunnett' test). (D) NIK inhibition attenuates NF-κB signaling. siRNA silencing of NIK but not the non-specific control siRNA, led to a decrease in NIK protein expression. RPMI-8226-NIK and 8226/R5-NIK were electroporated with control siRNA or with NIK siRNA. After 24-h cytoplasmic and nuclear extracts from transfected and untransfected cells were prepared. Cytoplasmic cell lysates were immunoblotted against NIK, phospho-IKKα/β, p-NF-κB2 p100, p-IκB-α and tubulin as marker of cytoplasmic separation as well as loading control; nuclear extracts were immunoblotted against NF-κB p65, NF-κB1 p50, NF-κB2 p52, RelB and Histone H2B as nuclear loading control; bands were subjected to densitometric scanning and the number below each lane represents the relative amount of the indicated proteins normalized to Tubulin or Histone H2B expression. Graphs below represent DNA binding activity of the NF-κB p65, NF-κB1 p50, NF-κB2 p52 and RelB subunit from the same nuclear extracts; results were normalized to the untransfected control (Untr). Values represent mean±SD of three separate experiments. (*P<0.05 vs. control siRNA condition; Dunnett test).

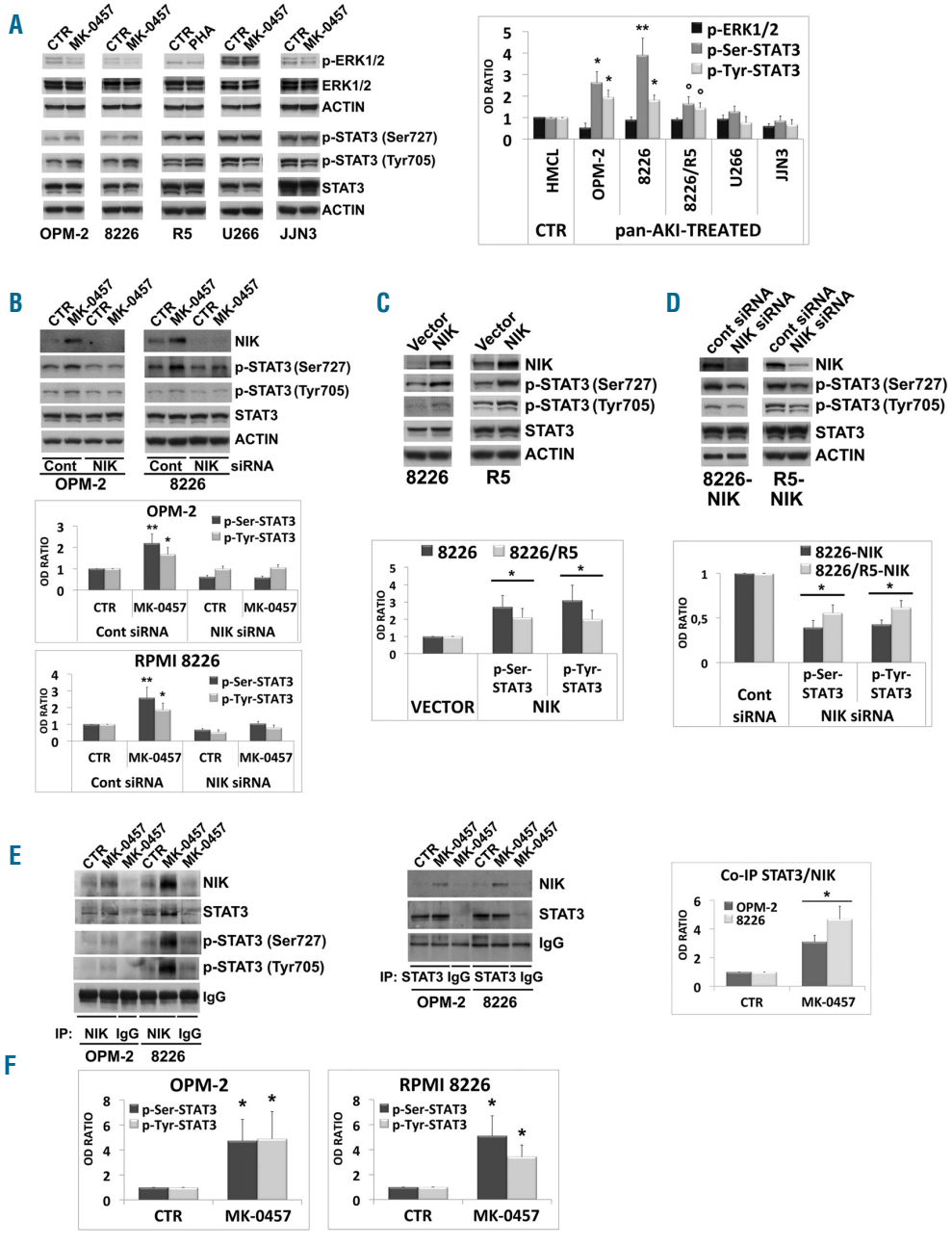

Figure 4. Pan-AKI-mediated accumulation of NF-κB-inducing kinase (NIK) induces STAT3 activation. (A) Wesern blot analysis of endogenous phospho-ERK1/2 (Thr202/Tyr204), ERK1/2 and Actin in MM cell lines treated with MK-0457 (0.4 μM) for 24 hours (h). The same lysates were prepared and immunoblotted against phospho-STAT3 (Ser727), phospho-STAT3 (Tyr705), STAT3 and Actin as loading control. Phospho-ERK1/2 and Ser727- and Tyr705-phosphorylated STAT3 were normalized to total ERK1/2 and STAT3 levels, respectively. In the graph, the phosphorylations under control conditions were set as 1 for comparison. In histogram are shown means±Standard Deviation (SD) of three independent experiments (°P<0.05, *P<0.01, **P<0.005 *vs.* control, Dunnett test). (B) OPM-2 and RPMI-8226 cells were transfected with NIK siRNA and after 3 h MM cell lines were treated with MK-0457 (0.4 μM). After 48 h whole cell lysates were prepared and immunoblotted against NIK, phospho-STAT3 (Ser727), phospho-STAT3 (Tyr705), STAT3 and Actin as loading control. Bands were subjected to densitometric scanning. STAT3 phosphorylations were normalized to overall STAT3 levels. STAT3 phosphorylations under untreated control condition were set to 1. Histograms below represent the mean±SD of three independent experiments. (*P<0.01, **P<0.005, Tukey-Kramer test). (C) Wesern blot analysis of NIK, phospho-STAT3 (Ser727), phospho-STAT3 (Tyr705), STAT3 and Actin in stable clones of RPMI-8226 and RPMI-8226/R5 transfected with empty vector or with plasmid expressing NIK. All western blotting results were evaluated by densitometric scanning, and histograms represent the relative levels of phospho-STAT3 corrected with respect to Actin and normalized to STAT3 expression. In the graph below, STAT3 phosphorylations under control conditions (empty vector transfection) were set as 1 for comparison. Histogram represents the mean±SD of five independent experiments. (*P<0.001 *vs.* empty vector, Dunnett test). (D) NIK expression of RPMI-8226-NIK and RPMI-8226/R5-NIK cells was inhibited by siRNA silencing; after 24 h cells were subjected to western blot analysis to monitor the expression of NIK, phospho-STAT3 (Ser727), phospho-STAT3 (Tyr705), STAT3 and Actin as loading control. Bands were subjected to densitometric scanning and STAT3 phosphorylations were normalized to total STAT3 levels. In the graph below, the relative fold change of protein levels was normalized with respect to the level of the control siRNA (cont), which was taken as 1. Histogram represents the mean±SD of five independent experiments (*P<0.001 *vs.* untreated control, Dunnett test). (E) OPM-2 and RPMI-8226 cell lines were treated with MK-0457 (0.4 μM) and after 24 h of treatment were lysed and subjected to immunoprecipitation (IP) using anti-NIK antibody or anti-STAT3 antibody or control antibody (IgG) and immunoblotted (IB) with either NIK or STAT3 antibodies. Western blot results were subjected to densitometric scanning and the histogram on the right shows average quantification results±SD of the association NIK/STAT3 from 3 immunoprecipitations (*P<0.0001 *vs.* untreated control cells, Dunnet and Tukey-Kramer tests). Anti-NIK immunoprecititate Filters stripped and reprobed for phospho-STAT3 (Ser727), phospho-STAT3 (Tyr705) and subjected to densitometric analysis (F); histograms represent the relative levels of phospho-STAT3 corrected with respect to IgG and normalized to STAT3 expression. STAT3 phosphorylations under control conditions were set as 1. Histograms show average quantification results±SD of three independent blots (*P<0.005, *vs.* untreated control cells, Dunnett and Tukey-Kramer tests).

alone or in co-culture with HS-5 stromal cells (Figure 2A). Importantly, NIK-in synergized with pan-AKI to kill MM cells (Figure 2B and *Online Supplementary Table S1*). Furthermore, adherence of MM cells to HS-5 stromal cells conferred significant protection against pan-AKI-induced cell death in the majority of the HMCL analyzed. However, this protective effect was significantly reduced by NIK inhibition (Figure 2A), thus confirming the important role of NIK in the stroma-mediated pan-AKI protection. Finally, NIK-in significantly (P<0.005; n=10) increased the cytotoxicity of pan-AKI in patient-derived primary MM cells (Figure 2C and *Online Supplementary Figure S2A*), with no significant differences in the response rates between newly diagnosed (n=3) and relapsed (n=7) patients (*Online Supplementary Figure S3*) but not on PBMC from healthy individuals (Figure 2C and *Online Supplementary Figure S2B*). These observations thereby indicate that NIK plays an important role in the responsiveness of MM cells to pan-AKI. (Patients' demographic and clinical characteristics are summarized in *Online Supplementary Table S2*).

It is also important to highlight the fact that treatment of MM cells with the proteasome inhibitor bortezomib (currently the standard of care for MM) caused a strong accumulation of the NIK protein in the majority of the HMCL analyzed (*Online Supplementary Figure S4A*) and its chemical inhibition significantly enhanced the anti-myeloma effects of bortezomib, thereby indicating that NIK can influence the sensitivity of MM cells to this drug (*Online Supplementary Figure S4B*).

NF-κB-inducing kinase interferes with the inhibitory activity of pan-AKI on NF-κB-inducing kinase

To examine whether NIK accumulation induced by pan-AKI counteracts their ability to inhibit NF-κB pathways in MM cells, we blocked its function with a NIK-specific siRNA and monitored NF-κB activity in response to pan-AKI. We found that in 4 of 5 HMCL tested (except OPM-

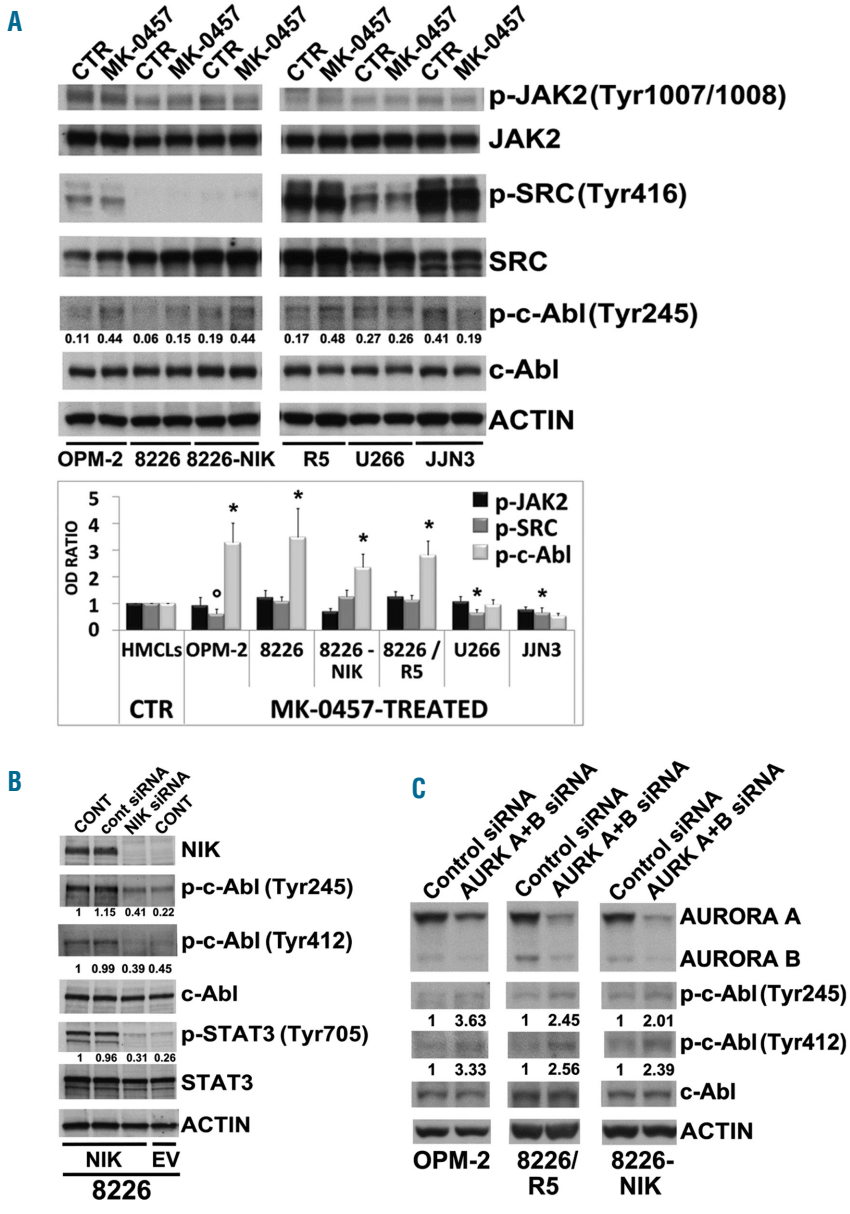

Figure 5. NF-κB-inducing kinase (NIK) accumulation induces c-Abl activation. (A) Western blot analysis of phospho-JAK2 (Tyr1007/1008), JAK2, phospho-SRC (Tyr416), SRC, phospho-c-Abl (Tyr245) and c-Abl kinases in multiple myeloma (MM) cell lines treated with MK-0457 (0.4 μM) for 24 hours (h); anti-Actin was performed as loading control. Bands were then subjected to densitometric scanning and levels of phospho-JAK2 (Tyr1007/1008), phospho-SRC (Tyr416), and phospho-c-Abl (Tyr245) were normalized to total JAK2, SRC, and c-Abl levels. Densitometric values of the ratio of phosphorylated c-Abl/total c-Abl are shown below the blots. The graph below represents the phosphorylation status of JAK2, SRC and c-Abl; changes (folds increase or decrease) in the levels of each phosphorylated protein relative to untreated control was taken as 1 (mean±Standard Deviation (SD) of 3 independent blots; °P<0.01, *P<0.005, *vs.* untreated control cells, Dunnett test). (B) NIK expression of RPMI-8226-NIK cells was inhibited by siRNA silencing; after 24 h transfected and untransfected cells were subjected to western blot analysis to monitor the expression of NIK, phospho-c-Abl (Tyr245), phospho-c-Abl (Tyr412), c-Abl, phospho-STAT3 (Tyr705), STAT3 and Actin as loading control. Protein expression of siRNA transfected 8226-NIK cells was compared to empty vector (EV) transfected control 8226 cells. Bands were then subjected to densitometric scanning: c-Abl and STAT3 phosphorylations were normalized to total c-Abl and STAT3 levels, respectively. The relative fold change of protein levels was normalized with respect to 8226-NIK untransfected condition, which was taken as 1 and are reported under each blot. (C) MM cell lines were transfected with siRNA against Aurora A and Aurora B (AURK A+B) or control siRNA. After 48 h transfected MM cell lines were subjected to western blot analysis to monitor the expression of Aurora A and B, phospho-c-Abl (Tyr245), phospho-c-Abl (Tyr412), c-Abl and Actin as loading control. c-Abl phosphorylations were subjected to densitometric scanning and were normalized to c-Abl levels. The relative fold change of protein levels was normalized with respect to the level of the untreated control, which was taken as 1, and is shown under each lane.

2 cells that have low NF-κB index[3,4,25]), NIK knockdown reduced the basal phosphorylation/activation status of IKKα and IKKβ (p-IKKα/β) and their respective downstream direct targets NF-κB2/p100 and IκB-α (Figure 3A), thus confirming that NIK affects not only the non-canonical but also the canonical NF-κB pathway in MM cells.[2-4] Notably, pan-AKI were ineffective (OPM-2) or only partially effective (all the other HMCL analyzed) in attenuating NF-κB signaling[25] (Figure 3A), and their reduced inhibitory activity on NF-κB signaling was closely linked to NIK induction because its knockdown by siRNA completely abrogated the pan-AKI-induced NF-κB activation in OPM-2 as well as greatly enhanced the pan-AKI-induced NF-κB inhibition in all the other HMCL analyzed (Figure 3A).

In support of these data, we found that experimental overexpression of NIK in MM cells (Figure 3B) caused enhanced phosphorylation of IKKα/β, NF-κB2/p100 and IκB-α, and increased nuclear localization and DNA binding activities of the NF-κB p65, p50, p52, and RelB subunits (Figure 3C). In contrast, NIK knockdown in these NIK-over-expressing MM cells consistently and significantly decreased their basal NF-κB activity (Figure 3D), thus confirming the important role of NIK in controlling NF-κB signaling in MM.[3,4]

NF-κB-inducing kinase induction by pan-AKI activates the STAT3 signaling pathway in multiple myeloma cells

Because NIK induction by pan-AKI was not associated with an increased activation of NF-κB pathways in 4 of 5 HMCL tested (except OPM-2), and yet NIK signaling has been demonstrated to crosstalk at different levels with other important prosurvival signaling pathways including MEK-ERK and STAT3 pathways,[8-10] we explored whether NIK induction by pan-AKI affected these pathways in MM cells.

Because NIK can phosphorylate MEK1 and thereby cause activation of downstream MAPK ERK,[9] we investigated whether NIK induction by pan-AKIs is associated with increased phosphorylation/activation of ERK in MM cells.

We found no significant change (U266, R5) or even a decrease (OPM-2, JJN3) in ERK activity (p-ERK1/2) in the pan-AKIs-treated HMCL (Figure 4A), thereby indicating that NIK, stabilized by pan-AKI, does not act through this pathway. Because STAT3 activity is regulated by two independent phosphorylations, one occurring at Tyr705 and one at Ser727, which are both required for it to be fully functional,[37] we specifically analyzed the STAT3 (Tyr705) and STAT3 (Ser727) phosphorylation patterns alongside with the overall protein expression levels. We found that treatment with pan-AKI significantly increased both Ser727 and Tyr705 STAT3 phosphorylation in OPM-2, RPMI-8226 and 8226/R5, but not in U266 and JJN3 HMCL where no significant changes in p-Ser-STAT3 or a decrease in p-Tyr-STAT3 phosphorylation were observed (Figure 4A).

Notably, NIK knockdown in MM cells completely abrogated both Ser727 and Tyr705 STAT3 phosphorylation induced by pan-AKI (Figure 4B), which would suggest that NIK is involved in the pan-AKI-mediated STAT3 activation. Confirming these data, we found that ectopic expression of NIK in MM cells caused enhanced phosphorylation of STAT3 in both serine and tyrosine residues (Figure 4C), whereas its depletion in these NIK-over-expressing MM cells consistently and significantly (P<0.001) decreased their basal STAT3 activity levels (Figure 4D).

In the light of evidence supporting reciprocal regulatory mechanisms and crosstalk between the NIK and STAT3 proteins,[10] we examined whether NIK exists in a complex with STAT3 in MM cells. Co-immunoprecipitation showed that STAT3 was associated with NIK and that this association was significantly enhanced by pan-AKI treatment of the cells (Figure 4E).

We also examined the Ser727 and Tyr705 phosphorylation state of STAT3 that co-immunoprecipitated with NIK and found that treatment with pan-AKI promoted a strong increase in the phosphorylation of NIK-associated STAT3 in both serine and tyrosine residues (Figure 4E and F), stressing the putative function of NIK in controlling STAT3 activation.

Aurora kinases inhibitors induce a NF-κB-inducing kinase dependent cytoplasmic relocalization and activation of c-Abl and promote the formation of the NIK-c-Abl-STAT3 ternary complex in multiple myeloma

Given the high levels of tyrosine-phosphorylated STAT3 that co-immunoprecipitates with the serine/threonine kinase NIK in response to pan-AKI treatment, we explored whether pan-AKI affect the Stat3 upstream tyrosine kinases JAK2, Src and/or c-Abl[38] activity/expression.

We found that, depending on the HMCL examined, pan-AKI caused a decrease or no significant changes in the Tyr-phosphorylation/activity of JAK2 (p-JAK2) and Src (p-SRC) kinases (Figure 5A), whereas they were able to significantly activate c-Abl in 4 of 6 HMCL tested (except U266 and JJN3 in which no significant changes or a decrease in c-Abl tyrosine-phosphorylation levels were observed, respectively) (Figure 5A). A significant increase (>3-fold) in p-c-Abl, but not in p-JAK2 and p-Src, was also observed in untreated 8226-NIK as compared to untreated 8226 HMCL (Figure 5A, lane 5 *vs.* lane 3). This finding links NIK to c-Abl signaling and, indeed, experimental overexpression of NIK in MM cells causes enhanced phosphorylation of endogenous c-Abl on Tyr245 and Tyr412 residues (both commonly used as Abl activation markers),[16,17] as well as Tyr705 phosphorylation of STAT3. Conversely, knockdown of NIK in these NIK-over-expressing MM cells consistently and significantly decreased their basal tyrosine-phosphorylation levels (Figure 5B). Accordingly, abrogation of Aurora-A and -B induced c-Abl phosphorylation at both Tyr245 and Tyr412 residues in MM cells (Figure 5C).

As c-Abl may exhibit both pro- and antiapoptotic functions depending on the subcellular localization (nuclear or cytoplasmic),[15-18] and its intracellular localization is regulated by phosphorylation of its Thr735 residue promoting cytoplasmic sequestration by the 14-3-3 protein,[19] we explored whether pan-AKI affect Thr735 phosphorylation and/or subcellular localization of c-Abl in MM cells in which the pervasive DNA damage leads to a predominantly nuclear localization of c-Abl.[21,22] As shown in Figure 6 and *Online Supplementary Figure S5*, endogenous c-Abl was predominantly accumulated in the nucleus of the MM cells,[21] while pan-AKI were able to cause a significant translocation of c-Abl from the nucleus to cytoplasm, thus elevating its cytoplasm/nucleus ratio in 4 of 5 HMCL tested (except JJN3) (Figure 6). Notably, the pan-AKI-induced cytoplasmic accumulation of c-Abl was associated with increased Thr735 phosphorylation of the cytoplasmic fraction of c-Abl (Figures 6 and 7A).

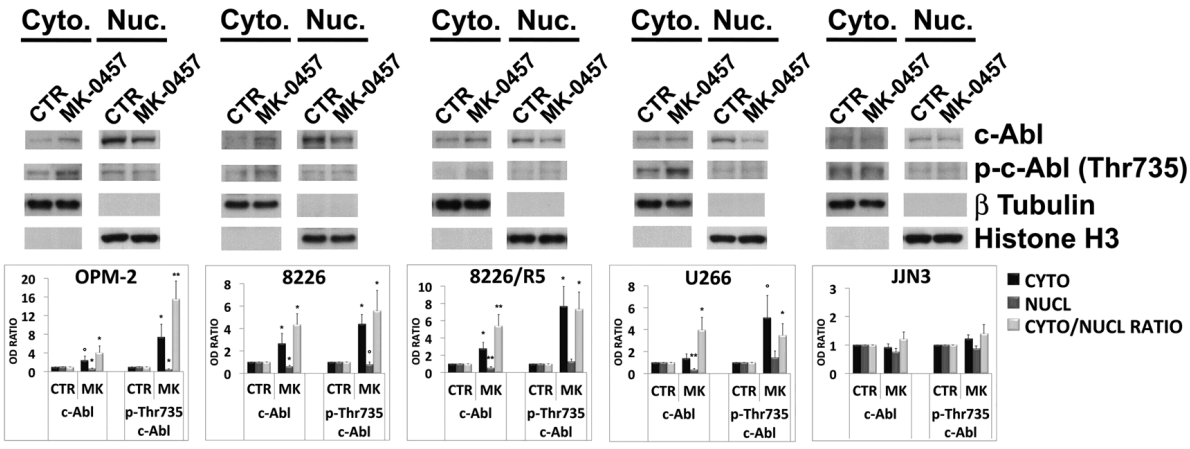

Figure 6. Aurora kinases inhibitors induce a cytoplasmic relocalization of c-Abl. Multiple myeloma (MM) cell lines were treated with MK-0457 (0.4 μM) and after 24 hours (h) cytoplasmic and nuclear extracts were prepared. Equal amount of Cytoplasmic (cyto) and nuclear (nuc) cell lysates (10 μg) were immunoblotted against c-Abl, phospho-c-Abl (Thr735), β Tubulin and Histone H3 as loading control of cytoplasmic and nuclear fraction, respectively. Bands were subjected to densitometric scanning: cytoplasmic and nuclear blots were normalized to total β Tubulin and Histone H3, respectively. The densitometric analysis is reported in the graphs below: the relative fold change of cytoplasmic or nuclear c-Abl and phospho-c-Abl (Thr735) levels was normalized with respect to control condition, which was taken as 1. The ratio of cytoplasmic to nuclear c-Abl and phospho-c-Abl (Thr735) protein expression (Cyto/Nuc) is shown. The c-Abl and phospho-c-Abl (Thr735) Cyto/Nuc ratio in untreated cells was set as 1. In the histograms are shown average quantification results±Standard Deviation (SD) of four independent blots (°P<0.05, *P<0.005, **P<0.001 *vs.* untreated control cells, Dunnett test).

Both processes, Thr735 phosphorylation and concomitant cytoplasmic accumulation of c-Abl, were closely linked to NIK induction since its overexpression in MM cells increased Thr735 phosphorylation of cytoplasmic c-Abl (Figure 7A) and caused c-Abl to translocate from the nuclear to the cytoplasmic compartment, whereas its inhibition in these NIK-over-expressing cells reversed this shuttling (Figure 7A). These data were further confirmed by immunofluorescence analysis (*Online Supplementary Figure S6*).

A closer examination revealed that NIK was diffused in the cytoplasm with an accumulation around the nucleus of the tumor cells treated with pan-AKI (Figure 7B), and its overexpression also caused enhanced tyrosine phosphorylation of cytoplasmic c-Abl (Figure 7A), to elicit its anti-apoptotic functions.[15-18]

Together with these results, siRNA-mediated knockdown of NIK completely abrogated the pan-AKI-induced Thr735 phosphorylation of c-Abl in OPM-2 and greatly decreased the high basal c-Abl Thr735 phosphorylation in the high NIK expressing JJN3 HMCL (Figure 7C).

Because pan-AKI can induce NIK accumulation and concomitant c-Abl activation, and both these kinases converge on and activate the STAT3 pathway,[10,17] we next investigated whether c-Abl can form a heterotrimeric complex with NIK and STAT3 in MM cells. As indicated in Figure 8A and B, there was little if any detectable interaction of c-Abl and NIK in untreated MM cells. However, exposure of MM cells to Pan-AKI led to an increase in the association of c-Abl with NIK kinases that was at least a 3-fold higher than in untreated control cells (Figure 8C).

The interaction between NIK and c-Abl, and that previously shown between NIK and STAT3 (Figure 4E), together with the fact that c-Abl can regulate the activation of STAT3 in cancer cells,[17] indicated that these three proteins may form a trimeric complexes in pan-AKI-treated MM cells. Accordingly, as shown in Figure 8B, immunoprecipitation of endogenous c-Abl from lysates of untreated or pan-AKI-treated MM cells followed by STAT3 immunoblotting revealed that the pharmacological blockade of Aurora kinases induced a physical interaction of c-Abl with STAT3, thus confirming that, in MM cells, pan-AKI can promote the formation of the ternary complex NIK-c-Abl-STAT3.

Pharmacological blockade of c-Abl sensitizes multiple myeloma cells to pan-AKI

To examine the functional significance of the pan-AKI-induced activation of c-Abl in MM cells we blocked its function using the Abl kinase inhibitors imatinib or nilotinib[20] and monitored cell death in response to pan-AKI treatment. Both imatinib or nilotinib significantly increased the pan-AKI-induced cell death in the majority of the HMCL as well as in patient-derived primary MM cells, (P<0.005; n=9) (Figure 9A and B and *Online Supplementary Figure S7A* and *B*), with no significant differences observed in the response rates of newly diagnosed (n=4) *versus* relapsed (n=5) patients (*Online Supplementary Figure S8*) and no effects seen in normal PBMC (Figure 9B and *Online Supplementary Figure S7C*).

In agreement with these results, Aurora-A and -B inhibition by either Aurora A/B-specific siRNA or AMG-900,[23,29] a potent and highly selective pan-AKI, significantly enhanced the sensitivity of MM cells to c-Abl inhibitors (Figure 9C, *Online Supplementary Figures S9* and *S10A* and *B*). Furthermore, c-Abl kinase inhibitors consistently synergized with pan-AKI to induce cell death in MM cells (*Online Supplementary Figure S11* and *Online Supplementary Table S3*).

Remarkably, as observed in the majority of the HMCL analyzed, treatment of cells isolated from MM patients with Pan-AKI induced NIK accumulation, increased Thr735, Tyr245 and Tyr412 phosphorylation of c-Abl and Ser727 and Tyr705 phosphorylation of STAT3 (Figure 9D). None of these conditions was observed in similarly treated PBMC from healthy donors.

To verify that the anti-tumor activity of pan-AKI and the synergizing effects of c-Abl inhibitors observed on cultured/isolated MM cells could be reproduced *in vivo*, we set up a multidrug-resistant xenograft mouse model of human MM. Consistent with our *in vitro* results, imatinib significantly potentiated the anti-tumor activity induced by pan-AKI in this *in vivo* setting, while having no effect as a single agent *in vivo* in a multidrug-resistant xenograft mouse model of human MM (Figure 10A). Animal survival was also significantly improved in mice treated with the combination imatinib/pan-AKI *versus* those that received monotherapies or vehicle alone ($P<0.0015$) (Figure 10A and *Online Supplementary Table S4*).

Immunobloting analyses on tumor masses harvested after five days post treatment confirmed decreases in the phosphorylation levels of Aurora kinases, enhancement of

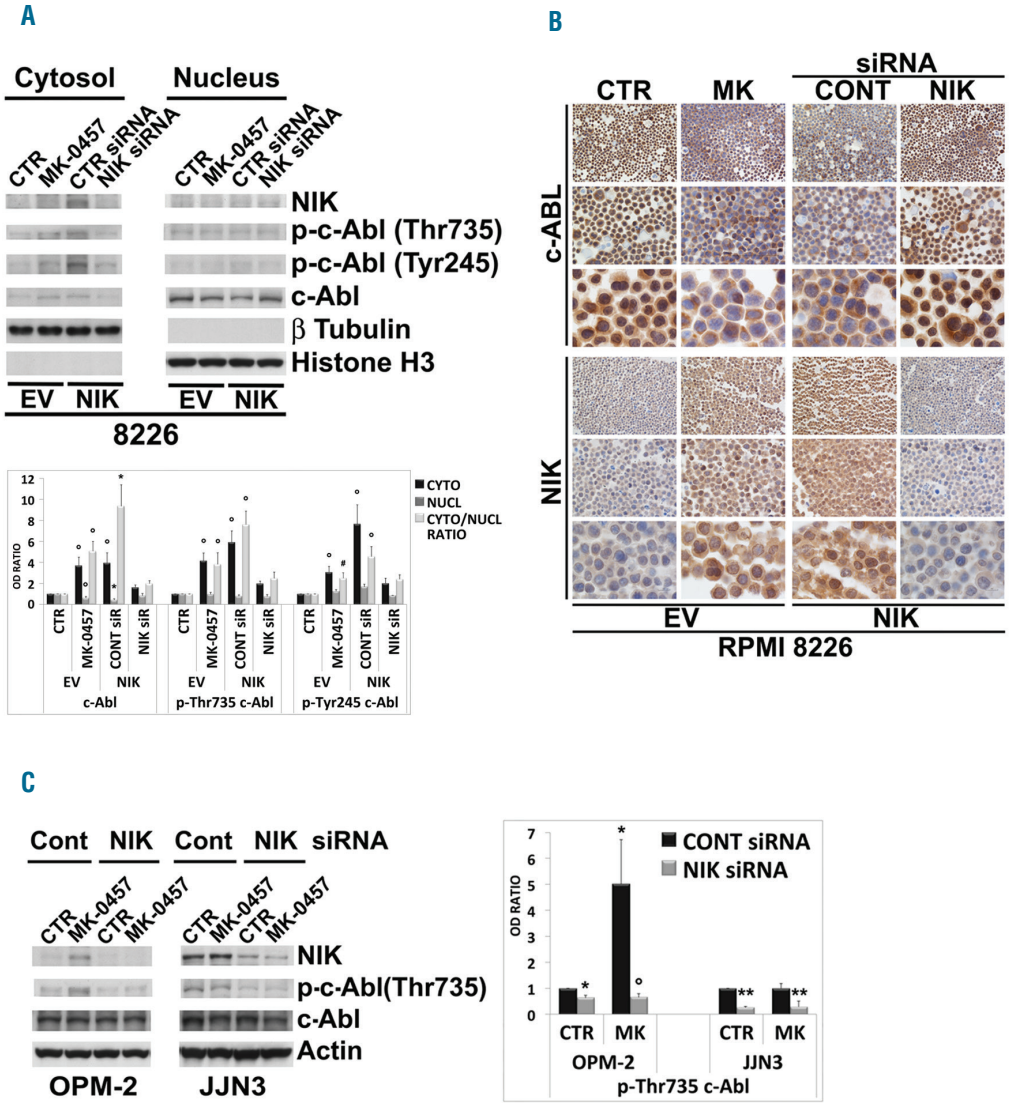

Figure 7. Accumulted NF-κB-inducing kinase (NIK) activates cytoplasmic c-Abl. (A) Stable clones of RPMI-8226 transfected with empty vector (EV) or with plasmid expressing NIK (NIK) were treated with MK-0457 (0.4 μM) or NIK siRNA, respectively. After 24 hours (h) cytoplasmic and nuclear extracts were prepared and equal amount of Cytoplasmic (cyto) and nuclear (nuc) cell lysates (10 μg) were immunoblotted against NIK, phospho-c-Abl (Thr735), phospho-c-Abl (Tyr245), c-Abl, β Tubulin and Histone H3 as loading control of cytoplasmic and nuclear fraction, respectively. Bands were subjected to densitometric scanning: cytoplasmic and nuclear blots were normalized to total β tubulin and Histone H3, respectively. In the graph below the relative fold change of cytoplasmic or nuclear c-Abl, phospho-c-Abl (Thr735) and phospho-c-Abl (Tyr245) levels was normalized with respect to empty vector (EV) control condition, which was taken as 1. The ratio of cytoplasmic to nuclear c-Abl, phospho-c-Abl (Thr735) and phospho-c-Abl (Tyr245) protein expression (Cyto/Nuc) is shown. The Cyto/Nuc ratio of phosphorylated and non-phosphorylated c-Abl in empty vector (EV) control condition (CONT) was set as 1. In histogram are shown average quantification results±Standard Deviation (SD) of three independent blots [#$P<0.01$, °$P<0.005$, *$P<0.001$ *vs.* (EV) control condition, Dunnett test]. (B) Stable clones of RPMI-8226 transfected with empty vector (EV) untreated or treated with MK-0457 (0.4 μM) and of RPMI-8226 expressing NIK (NIK) electroporated with non-specific control siRNA (CONT) or with NIK siRNA were harvested after an incubation of 24 h for cytospins and stained for c-Abl or were formalin fixed and paraffin embedded in cytoblocks for NIK staining. The microphotographs shown are representative of similar observation in three independent experiments (20x, 40x and 100x original magnifications). (C) OPM-2 and JJN3 cells were transfected with non-specific control siRNA (Cont) or NIK siRNA and after 3 h multiple myeloma (MM) cell lines were treated with MK-0457 (0.4 μM). After 48 h whole cell lysates were prepared and immunoblotted against NIK, phospho-c-Abl (Thr735), c-Abl and Actin as loading control. Bands were subjected to densitometric scanning. Levels of Thr735-phosphorylated c-Abl were normalized to overall c-Abl levels and c-Abl phosphorylation under non-specific siRNA control condition was set to 1. Histogram below represents the mean±SD of three independent experiments. (°$P<0.02$, *$P<0.005$, **$P<0.0005$ *vs.* control siRNA condition, Dunnett test).

NIK protein, and increases in the Thr735, Tyr245 and Tyr412 phosphorylation of c-Abl and Tyr705 phosphorylation of STAT3 in the case of xenografted animals treated with pan-AKI when compared to vehicle-treated controls (Figure 10B). In addition, immunohistochemical staining of tumor lesions for NIK and c-Abl revealed that also *in vivo* pan-AKI were capable of causing cytoplasmic NIK accumulation, which was most prominent around the nucleus of the tumor cells (Figure 10C and *Online Supplementary Figure S12*), whereas c-Abl was observed to have been extensively translocated from the nucleus to the cytoplasm (Figure 10C).

Finally, immunohistochemical analysis of tumor lesions isolated from pan-AKI-treated animals consistently revealed a significant reduction in the phosphorylation of Histone H3 on Ser10 (Figure 10D), a protein known to be a physiological substrate of Aurora kinases and a cellular proliferation marker.[39] This result would be consistent with the retardation of tumor growth observed in pan-AKI-treated *versus* vehicle-treated mice (Figure 10A).

Notably, combined imatinib and pan-AKI treatment blunted the pan-AKI-induced tyrosine (but not threonine) phosphorylation of c-Abl (Figure 10B) and increased the levels of apoptosis (cleaved-PARP and -caspase-3 staining), relative to that seen with monotherapies and vehicle alone (Figure 10D); a result that agreed with the tumor regression and the improved survival rate observed in mice treated with the imatinib-Pan-AKI combination therapy (Figure 10A).

Pan-AKI-induced NF-κB-inducing kinase accumulation promotes survival signaling through PIM kinases activation

Consistent with the fact that NIK can elicit pro-survival signals in MM cells through activation of NF-κB and STAT3 pathways, we found that experimental overexpression of NIK in MM cells caused the induction of the antia-poptotic NF-κB/STAT3 regulated genes Bcl-xL, A1/Bfl-1, Mcl-1 and XIAP[40] (Figure 11A), all of which represent important targets for sensitizing MM cells to anticancer agents,[1] including pan-AKI.[25] NIK overexpression was also associated with upregulation of PIM1 and PIM2 (Figure 11A), both oncogenic, constitutively active serine/threonine kinases transcriptionally regulated either by NF-κB or STAT3, that mediate survival signaling through the phosphorylation and inactivation of Bad[32,41] (Figure 11A). In accordance with its role in controlling anti-apoptotic signal transduction events, NIK overexpression protected MM cells from pan-AKI-induced cell death, which was reversed by the chemical or genetic disruption of NIK functions (Figure 11B).

We further found that in 5 of 7 HMCL tested (except U266 and JJN3 cells), the pan-AKI-induced NIK-stabilization was associated with enhanced levels of PIM1 and PIM2 proteins, and phosphorylation of their direct downstream target Bad (Figure 11C and *Online Supplementary Figure S13*); RNA interference-mediated knockdown of NIK or the use of a NIK-inhibitor (NIK-in) prevented these increments (Figure 11C), thus confirming the role of NIK in PIM kinases induction in MM cells. Taken together with our previous findings (Figures 4-8), the observations also supported the existence of a NIK /c-Abl /STAT3 /PIM /Bad signaling axis in pan-AKI-treated MM cells.

Consistent with the fact that STAT3 can regulate the expression of PIM kinases,[32,41] we found that its inhibition by siRNA completely abrogated the pan-AKI-induced PIM1 and PIM2 upregulation in OPM-2, RPMI-8226 and RPMI-8226-NIK HMCL, and greatly decreased their basal levels in JJN3 cells (Figure 11D).

Loss-of-function of STAT3 by either siRNA or the small-molecule inhibitor STATTIC[42] significantly enhanced the pan-AKI sensitivity of MM cells (Figure 11D and *Online Supplementary Figure S14*), thereby indicating that STAT3 activated by pan-AKI acted as a prosurvival, antiapoptotic transcription factor in MM.

PIM kinases have been implicated in the regulation of MM cell proliferation, survival, and drug resistance.[43] Given this, we examined whether their inhibition affected the responses of MM cells to pan-AKI. PIM1/2 inhibition, by either the specific small-molecule inhibitor SMI-4a[44] or by PIM1/2-specific siRNA significantly increased the pan-AKI-induced cell death in all the HMCL tested either cultured alone or together with HS-5 cells, except for U266 and JJN3 (Figure 12A and B, and *Online Supplementary Figure S15*), in which pan-AKI failed to increase PIM kinases levels (*Supplementary Figure S14)*.

Furthermore, treatment of patient-derived MM cells, but not normal PBMC, with Pan-AKI led to an increment

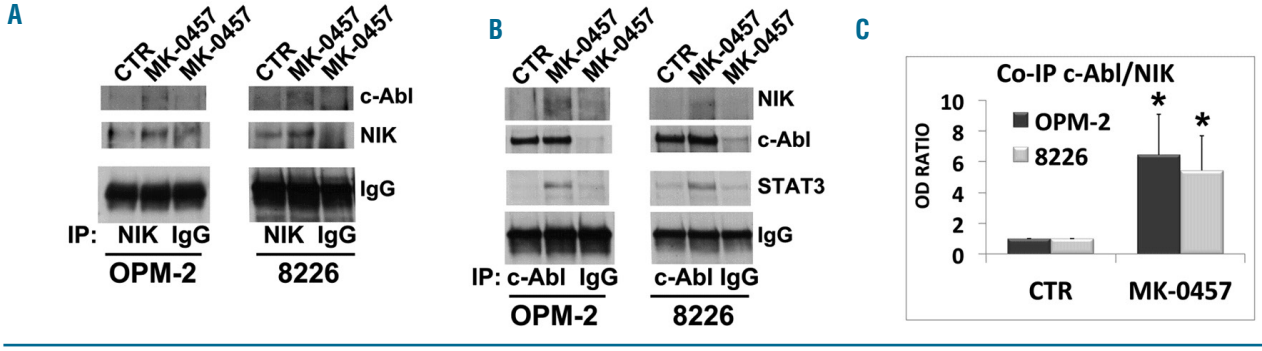

Figure 8. Accumulated NF-κB-inducing kinase (NIK) physically interacts with c-Abl and contributes to the NIK-c-Abl-STAT3 prosurvival complex formation. OPM-2 and RPMI-8226 cell lines were treated with MK-0457 at 0.4 μM and after 24 hours (h) of treatment were lysed and subjected to immunoprecipitation (IP) using (A) anti-NIK or (B) anti-c-Abl or control antibody (IgG) and immunoblotted (IB) with either NIK or c-Abl antibodies. Anti-c-Abl immunoprecititate filters were stripped and reprobed for STAT3. (C) Western blot of anti-NIK and anti-c-Abl immunoprecipitates results were subjected to densitometric scanning and protein expression under control conditions was set as 1. The histogram shows average quantification results±Standard Deviation (SD) of the association c-Abl/NIK from three immunoprecipitations (*P<0.001 *vs.* untreated control cells, Dunnett and Tukey-Kramer tests).

of PIM1/2 protein levels (Figure 12C), that significantly (P<0.005; n=10) influenced the responsiveness of the cells to pan-AKI, with similar response rates between newly diagnosed (n=3) and relapsed (n=7) patients (Figure 12D and *Online Supplementary Figures S2A* and *S3*), thereby indicating that these kinases may significantly impact on the susceptibility of MM cells to pan-AKI exposure.

Discussion

The critical role of NIK in regulating non-canonical and canonical NF-κB pathways in MM,[4-6] together with the fact that NIK and Aurora kinases can converge on common targets,[24-26] prompted us to hypothesize that NIK might interfere with and reduce or bypass the NF-κB inhibitory effects exerted by pan-AKI on MM cells. In support of this hypothesis, we found that pan-AKI induce NIK protein stabilization and that this depended on the downregulation of the TRAF2 protein, one of the critical NF-κB negative regulators that, together with TRAF3, form a molecular bridge that couples NIK to the NIK K48-ubiquitin ligase cIAP1/2.[6,7] We also found that TRAF2 reduction was sufficient to elevate NIK protein levels in MM cells harboring alterations in the TRAF3-binding domain of NIK or in TRAF3 itself, thus confirming that TRAF2 can regulate NIK stabilization independent of TRAF3.[4,45]

Although experimental overexpression of NIK led to a marked activation of both NF-κB and STAT3 pathways, its induction by pan-AKI resulted in the activation of only the STAT3 pathway, thereby suggesting that Aurora kinases

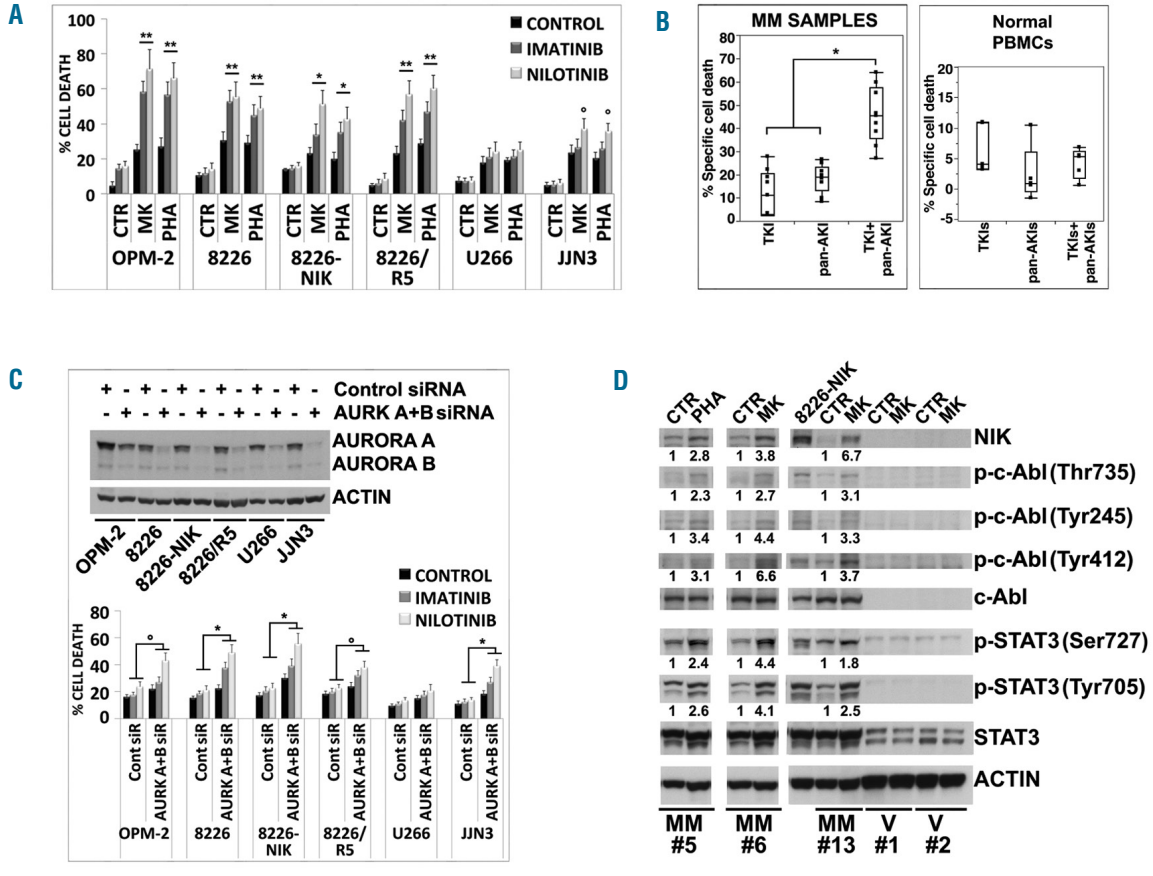

Figure 9. Pharmacological inhibition of Abl kinase enhances cytotoxicity induced by Aurora inhibition. (A) Multiple myeloma (MM) cell lines were incubated with imatinib and nilotinib at 2 μM for 3 hours (h), and were then treated with MK-0457 (0.4 μM) and PHA-680632 (1 μM). After 48 h the cell death was measured by sub-G1 DNA content and Annexin-V method. Values represent means±Standard Deviation (SD) of four independent experiments. (°P<0.05, *P<0.005, **P<0.001 *vs.* either treatment alone; Dunnett and Tukey-Kramer tests). (B) CD138-purified plasma cells from nine patients with MM seeded in presence of HS-5 cells and peripheral blood mononuclear cells (PBMC) from five healthy volunteers were preincubated for 3 h with imatinib or nilotinib at 2 μM and then with MK-0457 (0.4 μM) or PHA-680632 (1 μM). After 24 h cell death was measured by annexin-V staining or sub-G1 DNA content. Because of heterogeneous levels of basal cell death, the data of all nine primary samples and PBMC tested are expressed as % of specific cell death with the formula % Specific cell death = 100 x (induced cell death−basal cell death)/(100−basal cell death) and are shown in box plot format (median line in box delimited by 25th and 75th (*P<0.005 *vs.* either treatment alone; Dunnett test). (C) MM cell lines were transfected with siRNA against Aurora A and Aurora B (AURK A+B) or unrelated non-specific control siRNA (Cont) and after 48 h MM cell lines were subjected to western blot analysis to monitor the expression of Aurora A and Aurora B and Actin. Twenty-four hours after siRNA transfection, MM cell lines were treated with imatinib or nilotinib at 2 μM. After 48 h of treatment cell death was measured by flow cytometry analysis of Annexin-V staining or sub-G1 DNA content. Values represent means±SD of three independent experiments. (°P<0.05, *P<0.005 vs. imatinib and nilotinib of Control siRNA conditions; Dunnett and Tukey-Kramer tests). (D) CD138-purified plasma cells from three patients with MM (samples MM#5, MM#6, MM#13) and PBMC from two healthy volunteers (samples V#1 and V#2) were incubated with MK-0457 (0.4 μM) or PHA-680632 (1 μM) and after 24 h were subjected to western blot analysis to monitor the expression of NIK, phospho-c-Abl (Thr735), phospho-c-Abl (Tyr245), phospho-c-Abl (Tyr412), c-Abl, phospho-STAT3 (Ser727), phospho-STAT3 (Tyr705), STAT3 and Actin. Bands were subjected to densitometric scanning and normalized to Actin. c-Abl and STAT3 phosphorylations were normalized to total c-Abl and STAT3, respectively. The relative fold change of protein levels was normalized with respect to the level of the untreated control, which was taken as 1, and is shown under each lane.

can significantly contribute to the basal NF-κB activity of MM cells and that their inhibition can partially compensate for the NIK-induced activation of NF-κB pathways.

In MM, the pervasive DNA damage triggers constitutive activation of the ATR/ATM-regulated DNA damage response proapoptotic network which in turn leads to a prominent and preferential nuclear localization of c-Abl. Here, however, it is unable to induce apoptosis because of disruption of the ABL-YAP1-p73 axis.[21] The nuclear accumulation of c-Abl in MM[21] may explain its marginal role in MM pathogenesis[46] and the therapeutic inefficacy of c-Abl inhibitors in monotherapy regimens or when used in com-

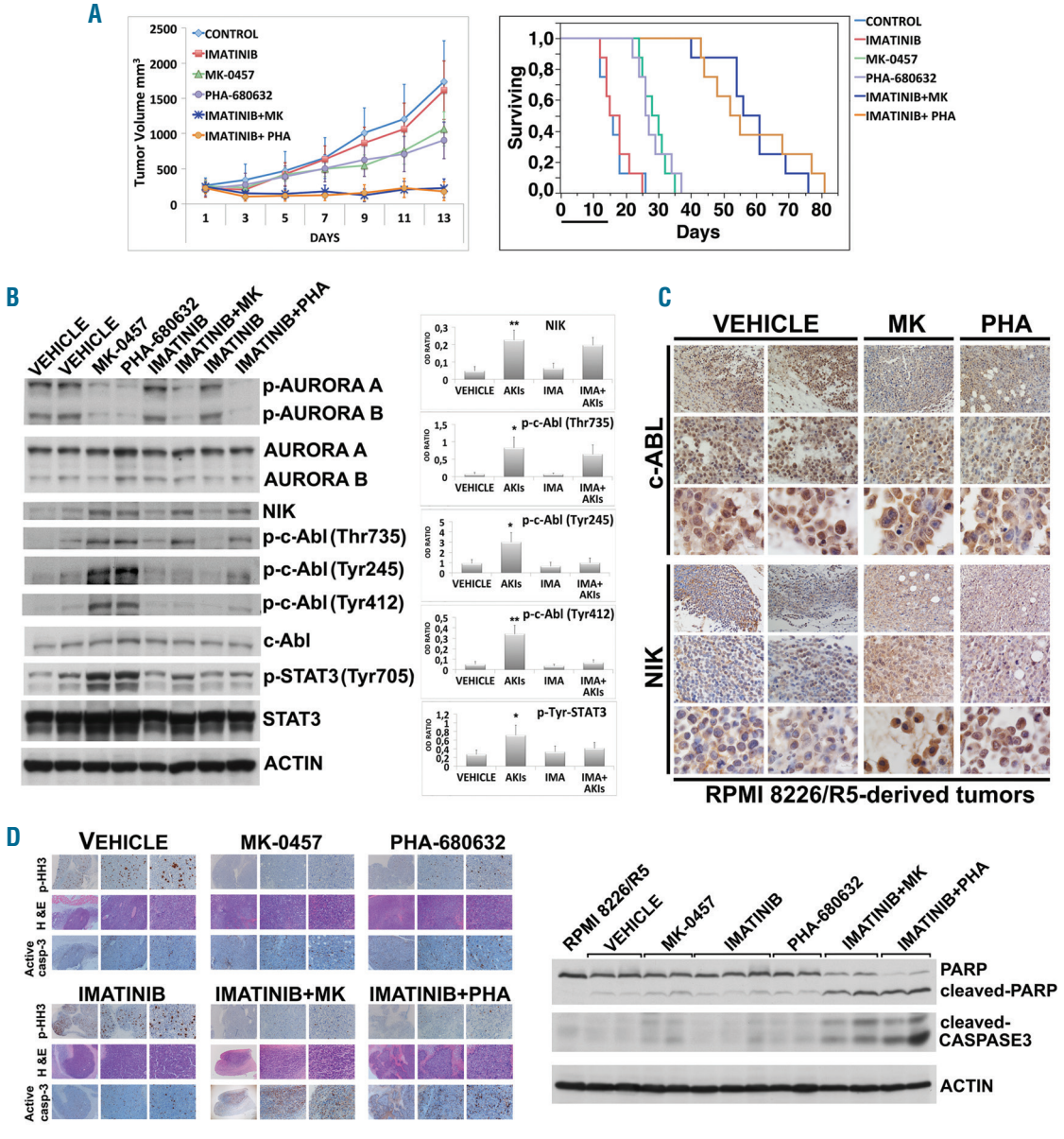

Figure 10. Pharmacological inhibition of Abl kinase improves the anti-myeloma effect of Aurora kinases inhibitors *in vivo*. (A) NOD-SCID mice were subcutaneously inoculated in the left flank with 10^7 RPMI-8226/R5 cells. When tumor size reached approximately 250 mm^3, mice were randomly assigned (n=12/group) to receive vehicle alone, MK-0457 (50 mg/kg), PHA-680632 (50 mg/kg), imatinib (50 mg/kg twice daily), or the combination imatinib/MK-0457 or imatinib/PHA-680632 for two weeks. Results are tumor volume, mean±Standard Deviation (SD) mm^3, plotted against time (P<0.001 imatinib/MK-0457 or imatinib/PHA-680632 *vs.* either treatment alone; Dunnett test). Kaplan-Meier survival curve was evaluated from the first day of treatment until death or sacrifice (P<0.0015, Log-Rank test after Bonferroni correction, imatinib/pan-AKI-treated animals vs. either treatment alone). The black bar on the abscissa represents the 14-day period of treatment. (B) After five days of treatment, four mice from each treatment group were humanely killed, and the tumors were removed for assay. Tumor tissues from mice were harvested and processed for western blot analysis to monitor phospho-Aurora A (Thr288), phospho-Aurora B (Thr232), Aurora A, Aurora B, NIK, phospho-c-Abl (Thr735), phospho-c-Abl (Tyr245), phospho-c-Abl (Tyr412), c-Abl, phospho-STAT3 (Tyr705), STAT3 and Actin as loading control. Bands were subjected to densitometric scanning and normalized to Actin. c-Abl and STAT3 phosphorylations were normalized to c-Abl and STAT3 levels, respectively. The blots shown are representative of similar observations in four different mice receiving the same treatment. Histograms show mean±Standard Deviation (SD) of densitometry results from four mice (*P<0.01, **P<0.001, Tukey-Kramer test). (C) Tumors from vehicle or pan-AKI treated mice were formalin fixed paraffin embedded and analyzed by immunohistochemical analysis of c-Abl and NIK. The microphotographs shown are representative of similar observation in four mice receiving the same treatment (20x, 40x and 100x original magnification). (D) RPMI-8226/R5-derived tumors were analyzed by immunohistochemical staining for phospho-Histone H3, hematoxylin and eosin (H&E), and cleaved caspase-3 (4x, 10x and 20x original magnification). The microphotographs shown are representative of similar observations in four different mice receiving the same treatment. Western blot analysis for PARP, cleaved-PARP, cleaved caspase-3 and Actin of representative mice from each treatment group; for comparison, cell lysate from RPMI-8226/R5 cells was loaded in the same gel.

bination with other agents for the treatment of MM.[47] Instead, by inducing a NIK-dependent cytoplasmic relocalization and activation of c-Abl, pan-AKI switch it from a pro-apoptotic to a pro-survival factor, thereby turning it into a potentially effective target for MM. In accordance with this, we demonstrate here that c-Abl inhibitors consistently increase the sensitivity of MM cells to pan-AKI in different experimental settings and in patient-derived cells.

Our data identify NIK as a kinase responsible for phosphorylation of c-Abl at Thr735, which is critical for its cytoplasmic retention, thereby indicating that NIK influences the subcellular localization of c-Abl in MM cells. NIK, stabilized by pan-AKI, forms a trimeric complex with c-Abl and STAT3 and, together with c-Abl, contributes to the serine 727 and tyrosine 705 phosphorylation of STAT3. NIK is also involved in the tyrosine-phosphorylation/ activation of c-Abl observed after pan-AKI treatment, as supported by our genetic perturbation experiments of NIK in MM cells. This recalls the fact that also serine/threonine kinases, in addition to SRC family kinases, may regulate the catalytic activity of c-Abl *via* direct protein-protein interactions and/or by promoting phosphorylation of c-Abl on serine and/or threonine residues.[16,17] Moreover, pan-AKI failed to induce c-Abl and STAT3 tyrosine phosphorylation in those HMCL (U266 and JJN3) in which the high basal activity of Src kinase

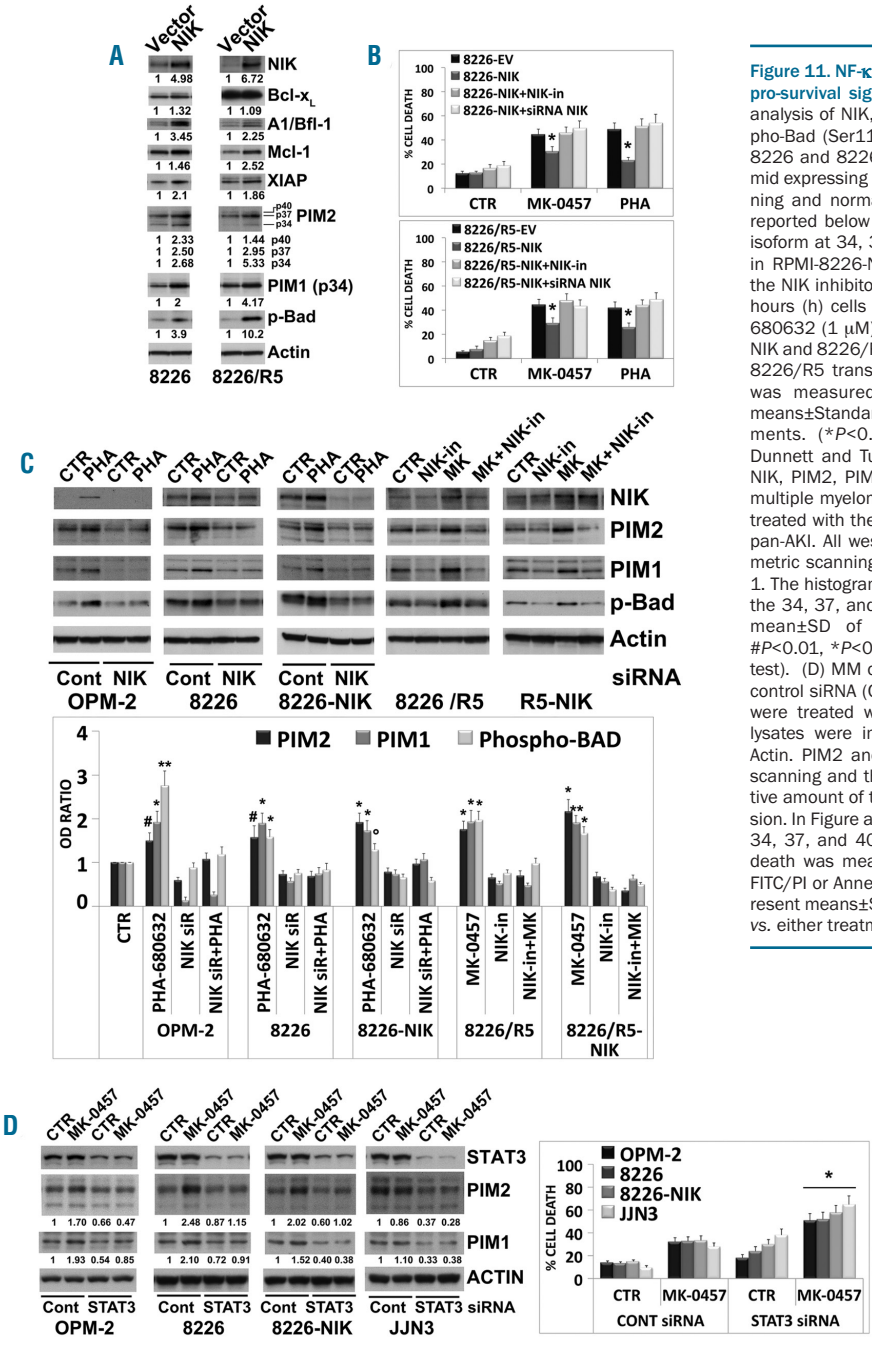

Figure 11. NF-κB-inducing kinase (NIK) accumulation promotes pro-survival signals by inducing PIM kinases. (A) Western Blot analysis of NIK, Bcl-xL, A1/Bfl-1, Mcl-1, XIAP, PIM2, PIM1, phospho-Bad (Ser112) and Actin proteins in stable clones of RPMI-8226 and 8226/R5 transfected with empty vector or with plasmid expressing NIK; bands were subjected to densitometric scanning and normalized relative fold change in protein levels are reported below each lane. Relative protein levels of each PIM2 isoform at 34, 37, and 40 kDa are reported. (B) NIK expression in RPMI-8226-NIK and 8226/R5-NIK cells was inhibited using the NIK inhibitor (NIK-in) at 10 μM or by siRNA silencing; after 3 hours (h) cells were treated with MK-0457 (0.4 μM) and PHA-680632 (1 μM). The cytotoxic effects of NIK inhibition of 8226-NIK and 8226/R5-NIK cells were compared to those of 8226 and 8226/R5 transfected with empty vector. After 72 h, apoptosis was measured by sub-G1 DNA content. Values represent means±Standard Deviation (SD) of three independent experiments. (*P<0.01 *vs.* Pan-AKI-treated NIK-expressing cells; Dunnett and Tukey-Kramer test). (C) Western blot analysis of NIK, PIM2, PIM1, phospho-Bad (Ser112) and Actin proteins in multiple myeloma (MM) cell lines transfected with NIK siRNA or treated with the NIK inhibitor (NIK-in) in presence or absence of pan-AKI. All western blotting results were evaluated by densitometric scanning and normalized to the untreated control set as 1. The histogram below shows combined densitometric values of the 34, 37, and 40 kDa PIM2 bands. Histogram represents the mean±SD of three independent experiments. (°P<0.05, #P<0.01, *P<0.005, **P<0.001 *vs.* untreated control, Dunnett test). (D) MM cell lines cells were transfected with non-specific control siRNA (Cont) or STAT3 siRNA and after 3 h MM cell lines were treated with MK-0457 (0.4 μM). After 48 h whole cell lysates were immunoblotted against STAT3, PIM2, PIM1 and Actin. PIM2 and PIM1 bands were subjected to densitometric scanning and the number below each lane represents the relative amount of the indicated proteins normalized to Actin expression. In Figure are reported combined densitometric values of the 34, 37, and 40 kDa PIM2 bands. At the same time point cell death was measured by flow cytometry analysis of Annexin V-FITC/PI or Annexin V-PE/7-AAD staining. Values in the graph represent means±SD of three independent experiments. (*P<0.005 *vs.* either treatment alone; Dunnett and Tukey-Kramer tests).

was significantly inhibited by pan-AKI, thereby indicating that Src kinase, of which c-Abl and STAT3 are direct downstream substrates and effectors,[16-18] may compensate for or obscure the pan-AKI-induced NIK-dependent c-Abl activation.

Based on its off-target activity against wild-type and mutated BCR-ABL including the imatinib-/nilotinib-/dasatinib-resistant T315I-BCR-ABL, MK-0457 has shown clinical efficacy in chronic myelogenous leukemia patients bearing T315I mutated BCR-ABL.[48-50] However, it has been

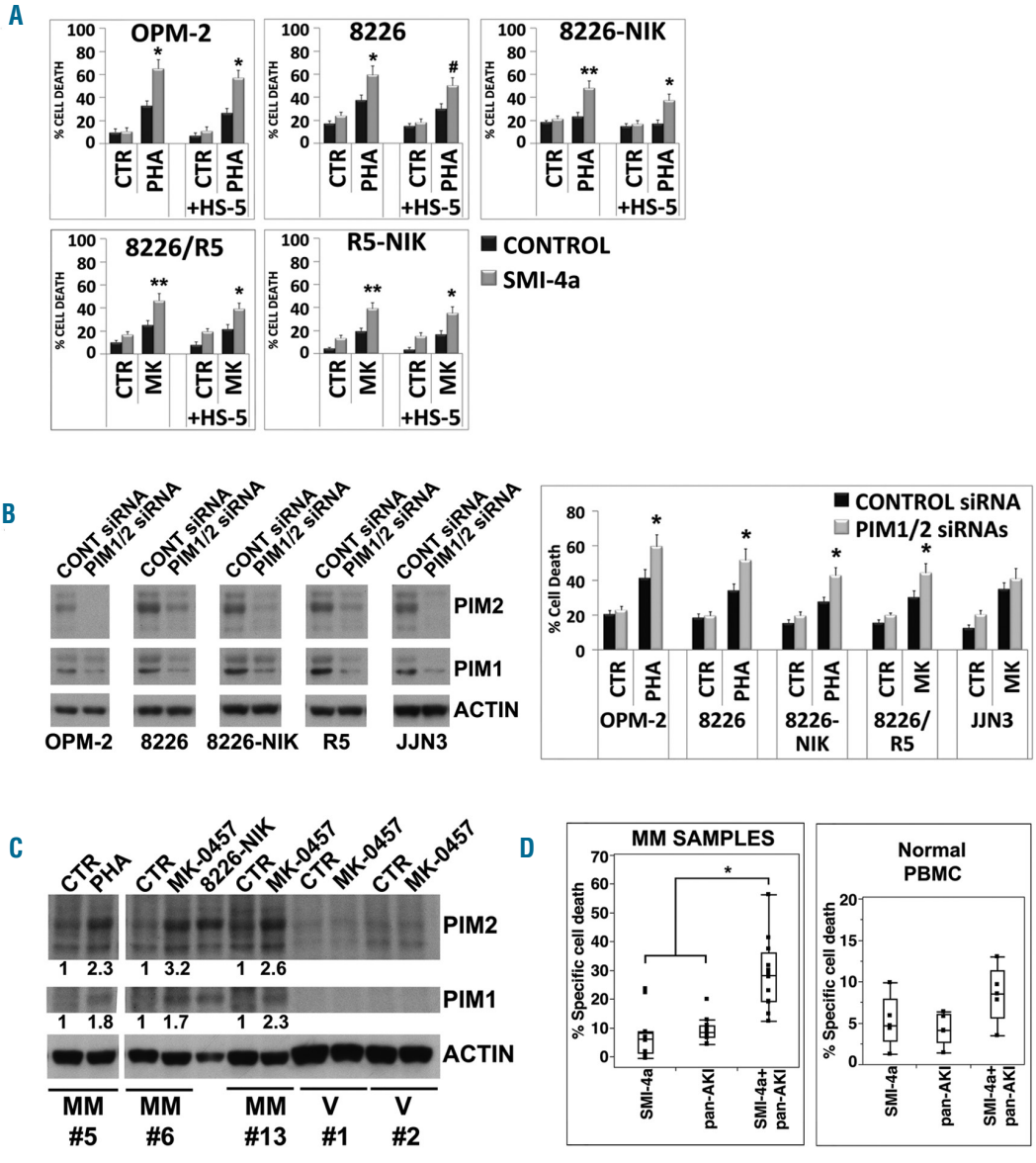

Figure 12. Functional inhibition of PIM kinases enhances the anti-myeloma effects of Aurora inhibitors. (A) Multiple myeloma (MM) cell lines were incubated with the pan-PIM kinase inhibitor (SMI-4a) at 10 μM for 3 hours (h), and then were treated with MK-0457 (0.4 μM) or PHA-680632 (1 μM) in absence or presence of HS-5 cells (+HS-5). After 48 h cell death was measured by flow cytometry analysis of Annexin V-FITC/PI or Annexin V-PE/7-AAD staining. Values represent means±Standard Deviation (SD) of three independent experiments. (#P<0.05, *P<0.01, **P<0.005 *vs.* pan-AKI-treated MM cell lines; Dunnett test). (B) MM cell lines cells were transfected with non-specific control siRNA (Cont) or cotransfected with siRNA targeting PIM1 and PIM2 and after 3 h MM cell lines were treated with MK-0457 (0.4 μM) or PHA-680632 (1 μM). After 48 h whole cell lysates of transfected MM cell lines were prepared and immunoblotted against PIM2, PIM1 and Actin. At the same time point, cell death was measured by flow cytometry analysis of Annexin V-FITC/PI or Annexin V-PE/7-AAD staining. Values in the graph represent means±SD of 3 independent experiments. (*P<0.05 *vs.* non-specific control siRNA; Dunnett and Tukey-Kramer tests). (C) PIM2, PIM1 and Actin western blot analysis in CD138-purified plasma cells from three patients with MM (samples MM#5, MM#6, MM#13) and peripheral blood mononuclear cells (PBMC) from two healthy volunteers (samples V#1, V#2) treated with pan-AKI. Bands were subjected to densitometric scanning and normalized to Actin; changes (folds increase) in the levels of each protein relative to untreated control, which was taken as 1 and values are shown below each lane. (D) CD138-purified plasma cells from ten patients with MM seeded in in presence of HS-5 cells and PBMC from five healthy volunteers were incubated with the pan-PIM kinase inhibitor (SMI-4a) at 10 μM for 3 h, and then with MK-0457 (0.4 μM) or PHA-680632 (1 μM). After 24 h cell death was measured by annexin-V staining and/or sub-G1 DNA content. Because of heterogeneous levels of basal cell death, the data of all ten primary samples and PBMC tested are expressed as % of specific cell death with the formula % Specific cell death = 100 x (induced cell death−basal cell death)/(100−basal cell death) and are shown in box plot format (median line in box delimited by 25th and 75th) (*P<0.005 *vs.* either treatment alone; Dunnett test).

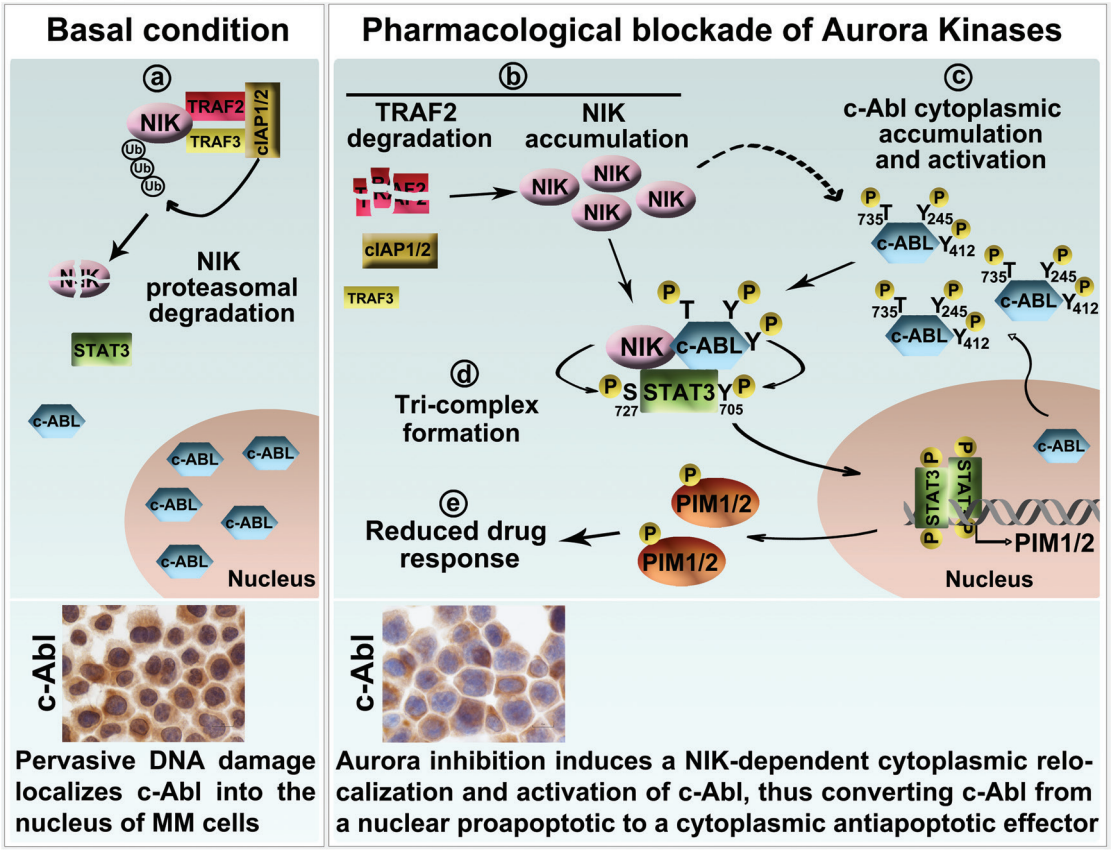

Figure 13. Schematic representation of our proposed molecular model for NIK/c-Abl/STAT3/PIM axis in multiple myeloma (MM) cells. (a) Under basal conditions, NF-κB-inducing kinase (NIK) is degraded through the TRAF2/TRAF3/cIAP1/2 complex and, because of constitutive DNA damage and activation of the DNA damage response network, c-Abl is primarily localized in the nucleus. (b) Upon treatment with Aurora kinase inhibitors TRAF2 is degraded and NIK accumulates. (c) Accumulated NIK induces cytoplasmic relocalization and activation of c-Abl by promoting its phosphorylation at Thr735, Tyr 245 and Tyr 412; (d) NIK and c-Abl co-operate to form a complex with and phosphorylate STAT3 at Ser727 and Tyr705, thus increasing its transcriptional activity and leading to the upregulation of the anti-apoptotic STAT3-target genes PIM1 and PIM2. (e) PIM induction reduces drug response; depletion or inactivation of any of the tri-complex components as well as PIM kinases potentiates the anti-myeloma activity of Aurora inhibitors.

demonstrated that MK-0457 is able to inhibit the autophosphorylation of T315I mutant BCR-ABL at concentrations (IC50 values ranging from 5 to 10 μM)[49,51,52] which are significantly higher than those clinically achievable (plasma/serum concentrations 1-3 μM)[48,50,53] and 12.5-100-fold greater than those required to inhibit Aurora kinases and exert its anti-tumor activities.[49,51] Particular attention was, therefore, given here to assay the effects of MK-0457 at submolar concentrations (0.1-0.4 μM) in all of our *in vitro* experiments.

Interestingly, MK-0457, in its cytostatic and/or cytotoxic potential, did not discriminate between parental and wild-type or mutants BCR-ABL-transformed Ba/F3 cells.[49,52] However, hematologic responses were also observed in patients treated with MK-0457 at clinical doses that had not been reported to affect BCR-ABL kinase activity.[50] This would suggest that the activity of the drug is mainly exerted through inhibition of Aurora kinases rather than by interference with BCR-ABL function.

Finally, a role for c-Abl in the activation of STAT3 has been reported,[13,38] as well as a connection between c-Abl and Mcl-1 in chronic myelogenous and lymphocytic leukemias.[13,54] Indeed, we have previously showed that pan-AKIs were capable of up-regulating Mcl-1 in MM cells.[25]

Thus, cytoplasmic relocalization and activation of c-Abl secondary to NIK cytoplasmic accumulation, together with the formation of NIK/c-Abl/STAT3 trimeric complexes, emerge as novel survival mechanisms that significantly impair the antitumor efficacy of pan-AKI and identify potential translational approaches for targeting these mechanisms by using pan-AKI in combination with NIK, c-Abl, STAT3 and/or PIM inhibitors (Figure 13).

Funding

This work was supported by grants from "Chiara Tassoni" Onlus Association, Parma, Italy (LM), Associazione Italiana per la Ricerca sul Cancro (IG, Rif 10670, Italian Association for Cancer Research, Milan, Italy; AB), and Fondazione Cassa di Risparmio di Parma (Cariparma, Parma, Italy; AB). This work was supported by the Italian Ministry of Health (GR-2016-02363646 to LM) and by Regione Emilia Romagna L. 20/2002 (GPG/2018/918 to PL).

References

1. Kuehl WM, Bergsagel PL. Molecular pathogenesis of multiple myeloma and its premalignant precursor. J Clin Invest. 2012; 122(10):3456-3463.
2. Keats JJ, Fonseca R, Chesi M, et al. Promiscuous mutations activate the noncanonical NF-kappaB pathway in multiple myeloma. Cancer Cell. 2007;12(2):131-144.
3. Annunziata CM, Davis RE, Demchenko Y, et al. Frequent engagement of the classical and alternative NF-kappaB pathways by diverse genetic abnormalities in multiple myeloma. Cancer Cell. 2007;12(2):115-130.
4. Demchenko YN, Glebov OK, Zingone A, Keats JJ, Bergsagel PL, Kuehl WM. Classical and/or alternative NF-kappaB pathway activation in multiple myeloma. Blood. 2010; 115(17):3541-3552.
5. Grech AP, Amesbury M, Chan T, Gardam S, Basten A, Brink R. TRAF2 differentially regulates the canonical and noncanonical pathways of NF-kappaB activation in mature B cells. Immunity. 2004;21(5):629-642.
6. Vallabhapurapu S, Matsuzawa A, Zhang W, et al. Nonredundant and complementary functions of TRAF2 and TRAF3 in a ubiquitination cascade that activates NIK-dependent alternative NF-kappaB signaling. Nat Immunol. 2008;9(12):1364-1370.
7. Varfolomeev E, Blankenship JW, Wayson SM, et al. IAP antagonists induce autoubiquitination of c-IAPs, NF-kappaB activation, and TNFalpha-dependent apoptosis. Cell. 2007;131(4):669-681.
8. Thu YM, Richmond A. NF- B inducing kinase: a key regulator in the immune system and in cancer. Cytokine Growth Factor Rev. 2010;21(4):213-226
9. Rangaswami H, Bulbule A, Kundu GC. Nuclear factor-inducing kinase plays a crucial role in osteopontin-induced MAPK/IkappaBalpha kinase-dependent nuclear factor kappaB-mediated promatrix metalloproteinase-9 activation. J Biol Chem. 2004;279(37):38921-38935.
10. Nadiminty N, Chun JY, Hu Y, Dutt S, Lin X, Gao AC. LIGHT, a member of the TNF superfamily, activates Stat3 mediated by NIK pathway. Biochem Biophys Res Commun. 2007;359(2):379-384.
11. Bharti AC, Shishodia S, Reuben JM, et al. Nuclear factor-kappaB and STAT3 are constitutively active in CD138+ cells derived from multiple myeloma patients, and suppression of these transcription factors leads to apoptosis. Blood. 2004;103(8):3175-3184.
12. Lee H, Herrmann A, Deng JH, et al. Persistently activated Stat3 maintains constitutive NF-kappaB activity in tumors. Cancer Cell. 2009;15(4):283-293.
13. Allen JC, Talab F, Zuzel M, Lin K, Slupsky JR. c-Abl regulates Mcl-1 gene expression in chronic lymphocytic leukemia cells. Blood. 2011;117(8):2414-2422.
14. Hilbert DM, Migone TS, Kopf M, Leonard WJ, Rudikoff S. Distinct tumorigenic potential of abl and raf in B cell neoplasia: abl activates the IL-6 signaling pathway. Immunity. 1996;5(1):81-89.
15. Pendergast AM. The Abl family kinases: mechanisms of regulation and signaling. Adv Cancer Res. 2002;85:51-100.
16. Brasher BB, Van Etten RA. c-Abl has high intrinsic tyrosine kinase activity that is stimulated by mutation of the Src homology 3 domain and by autophosphorylation at two distinct regulatory tyrosines. J Biol Chem. 2000;275(45):35631-35637.
17. Sirvent A, Benistant C, Roche S. Cytoplasmic signalling by the c-Abl tyrosine kinase in normal and cancer cells. Biol Cell. 2008;100(11):617-31.
18. Plattner R, Kadlec L, DeMali KA, Kazlauskas A, Pendergast AM. c-Abl is activated by growth factors and Src family kinases and has a role in the cellular response to PDGF. Genes Dev. 1999;13(18):2400-2411.
19. Yoshida K, Yamaguchi T, Natsume T, Kufe D, Miki Y. JNK phosphorylation of 14-3-3 proteins regulates nuclear targeting of c-Abl in the apoptotic response to DNA damage. Nat Cell Biol. 2005;7(3):278-285.
20. Greuber EK, Smith-Pearson P, Wang J, Pendergast AM. Role of ABL family kinases in cancer: from leukaemia to solid tumours. Nat Rev Cancer. 2013;13(8):559-571.
21. Cottini F, Hideshima T, Xu C, et al. Rescue of Hippo coactivator YAP1 triggers DNA damage-induced apoptosis in hematological cancers. Nat Med. 2014;20(6):599-606.
22. Walters DK, Wu X, Tschumper RC, et al. Evidence for ongoing DNA damage in multiple myeloma cells as revealed by constitutive phosphorylation of H2AX. Leukemia. 2011;25(8):1344-1353.
23. Otto T, Sicinski P. Cell cycle proteins as promising targets in cancer therapy. Nat Rev Cancer. 2017;17(2):93-115.
24. Briassouli P, Chan F, Savage K, Reis-Filho JS, Linardopoulos S. Aurora-A regulation of nuclear factor-kappaB signaling by phosphorylation of IkappaBalpha. Cancer Res. 2007;67(4):1689-1695.
25. Mazzera L, Lombardi G, Abeltino M, et al. Aurora and IKK kinases cooperatively interact to protect multiple myeloma cells from Apo2L/TRAIL. Blood. 2013;122(15):2641-2653.
26. Katsha A, Arras J, Soutto M, Belkhiri A, El-Rifai W. AURKA regulates JAK2-STAT3 activity in human gastric and esophageal cancers. Mol Oncol. 2014;8(8):1419-1428.
27. Katayama H, Wang J, Treekitkarnmongkol W, et al. Aurora kinase-A inactivates DNA damage-induced apoptosis and spindle assembly checkpoint response functions of p73. Cancer Cell. 2012;21(2):196-211.
28. Hose D, Rème T, Meissner T, et al. Inhibition of aurora kinases for tailored risk-adapted treatment of multiple myeloma. Blood. 2009;113(18):4331-4340.
29. Borisa AC, Bhatt HG. A comprehensive review on Aurora kinase: Small molecule inhibitors and clinical trial studies. Eur J Med Chem. 2017;140:1-19.
30. Hay AE, Murugesan A, DiPasquale AM, et al. A phase II study of AT9283, an aurora kinase inhibitor, in patients with relapsed or refractory multiple myeloma: NCIC clinical trials group IND.191. Leuk Lymphoma. 2016;57(6):1463-1466.
31. Rosenthal A, Kumar S, Hofmeister C, et al. A Phase Ib Study of the combination of the Aurora Kinase Inhibitor Alisertib (MLN8237) and Bortezomib in Relapsed Multiple Myeloma. Br J Haematol. 2016;174(2):323-325.
32. Nawijn MC, Alendar A, Berns A. For better or for worse: the role of Pim oncogenes in tumorigenesis. Nat Rev Cancer. 2011; 11(1):23-34.
33. Buzzeo R, Enkemann S, Nimmanapalli R, et al. Characterization of a R115777-resistant human multiple myeloma cell line with cross-resistance to PS-341. Clin Cancer Res. 2005;11(16):6057-6064.
34. Lunghi P, Giuliani N, Mazzera L, et al. Targeting MEK/MAPK signal transduction module potentiates ATO-induced apoptosis in multiple myeloma cells through multiple signaling pathways. Blood. 2008; 112(6): 2450-2462.
35. Li ZW, Chen H, Campbell RA, Bonavida B, Berenson JR. NF-kappaB in the pathogenesis and treatment of multiple myeloma. Curr Opin Hematol 2008;15(4):391-399.
36. Ranuncolo SM, Pittaluga S, Evbuomwan MO, Jaffe ES, Lewis BA. Hodgkin lymphoma requires stabilized NIK and constitutive RelB expression for survival. Blood. 2012;120(18): 3756-3763.
37. Wen Z, Zhong Z, Darnell JE Jr. Maximal activation of transcription by Stat1 and Stat3 requires both tyrosine and serine phosphorylation. Cell. 1995;82(2):241-250.
38. Fang B. Genetic Interactions of STAT3 and Anticancer Drug Development. Cancers (Basel). 2014;6(1):494-525.
39. Crosio C, Fimia GM, Loury R, et al. Mitotic phosphorylation of histone H3: spatio-temporal regulation by mammalian Aurora kinases. Mol Cell Biol. 2002;22(3):874-885.
40. Grivennikov SI, Karin M. Dangerous liaisons: STAT3 and NF-kappaB collaboration and crosstalk in cancer. Cytokine Growth Factor Rev. 2010;21(1):11-19.
41. Fox CJ, Hammerman PS, Cinalli RM, Master SR, Chodosh LA, Thompson CB. The serine/threonine kinase Pim-2 is a transcriptionally regulated apoptotic inhibitor. Genes Dev 2003;17(15):1841-1854.
42. Schust J, Sperl B, Hollis A, Mayer TU, Berg T. Stattic: a small-molecule inhibitor of STAT3 activation and dimerization. Chem Biol. 2006;13(11):1235-1242.
43. Asano J, Nakano A, Oda A, et al. The serine/threonine kinase Pim-2 is a novel anti-apoptotic mediator in myeloma cells. Leukemia. 2011;25(7):1182-1188.
44. Xia Z, Knaak C, Ma J, et al. Synthesis and evaluation of novel inhibitors of Pim-1 and Pim-2 protein kinases. J Med Chem. 2009; 52(1):74-86.
45. Döppler H, Liou GY, Storz P. Downregulation of TRAF2 mediates NIK-induced pancreatic cancer cell proliferation and tumorigenicity. PLoS One. 2013; 8(1):e53676.
46. Linden M, Kirchhof N, Kvitrud M, Van Ness B. ABL-MYC retroviral infection elicits bone marrow plasma cell tumors in Bcl-X(L) transgenic mice. Leuk Res. 2005;29(4):435-444.
47. Dispenzieri A, Gertz MA, Lacy MQ, et al. A phase II trial of imatinib in patients with refractory/relapsed myeloma. Leuk Lymphoma. 2006;47(1):39-42.
48. Weisberg E, Manley PW, Cowan-Jacob SW, Hochhaus A, Griffin JD. Second generation inhibitors of BCR-ABL for the treatment of imatinib-resistant chronic myeloid leukaemia. Nat Rev Cancer. 2007;7(5):345-356.
49. Carter TA, Wodicka LM, Shah NP, et al. Inhibition of drug-resistant mutants of ABL, KIT, and EGF receptor kinases. Proc Natl Acad Sci U S A. 2005;102(31):11011-11016.
50. Giles FJ, Swords RT, Nagler A, et al. MK-0457, an Aurora kinase and BCR-ABL inhibitor, is active in patients with BCR-ABL T315I leukemia. Leukemia. 2013;27(1):113-117.
51. Donato NJ, Fang D, Sun H, Giannola D, Peterson LF, Talpaz M. Targets and effectors of the cellular response to aurora kinase inhibitor MK-0457 (VX-680) in imatinib sensitive and resistant chronic myelogenous leukemia. Biochem Pharmacol. 2010; 79(5):688-697.
52. Shah NP, Skaggs BJ, Branford S, et al. Sequential ABL kinase inhibitor therapy selects for compound drug-resistant BCR-ABL mutations with altered oncogenic potency. J Clin Invest. 2007;117(9):2562-2569.
53. Traynor AM, Hewitt M, Liu G, et al. Phase I dose escalation study of MK-0457, a novel Aurora kinase inhibitor, in adult patients with advanced solid tumors. Cancer Chemother Pharmacol. 2011;67(2):305-314.
54. Aichberger KJ, Mayerhofer M, Krauth MT, et al. Identification of mcl-1 as a BCR/ABL-dependent target in chronic myeloid leukemia (CML): evidence for cooperative antileukemic effects of imatinib and mcl-1 antisense oligonucleotides. Blood. 2005; 105(8):3303-3311.